Since January 2020 Elsevier has created a COVID-19 resource centre with free information in English and Mandarin on the novel coronavirus COVID-19. The COVID-19 resource centre is hosted on Elsevier Connect, the company's public news and information website.

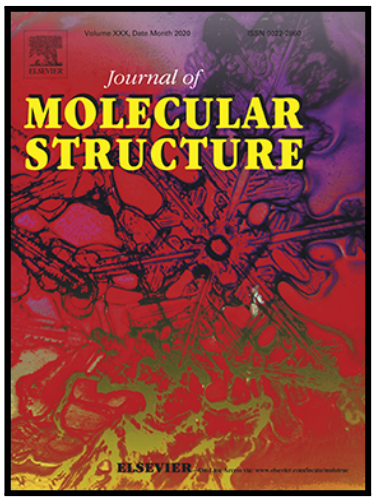

Synthesis, characterization, molecular docking, and anticancer activities of new 1,3,4-oxadiazole-5-fluorocytosine hybrid derivatives

Az-eddine El Mansouri , Saida Lachhab , Ali Oubella , Mehdi Ahmad , Johan Neyts , Dirk Jochmans , Winston Chiu , Laura Vangeel , Steven De Jonghe , Hamid Morjani , Mustapha Ait Ali , Mohamed Zahouily , Yogesh S. Sanghvi , Hassan B. Lazrek

PII: S0022-2860(22)01786-0
DOI: https://doi.org/10.1016/j.molstruc.2022.134135
Reference: MOLSTR 134135

To appear in: *Journal of Molecular Structure*

Received date: 7 June 2022
Revised date: 7 September 2022
Accepted date: 8 September 2022

Please cite this article as: Az-eddine El Mansouri , Saida Lachhab , Ali Oubella , Mehdi Ahmad , Johan Neyts , Dirk Jochmans , Winston Chiu , Laura Vangeel , Steven De Jonghe , Hamid Morjani , Mustapha Ait Ali , Mohamed Zahouily , Yogesh S. Sanghvi , Hassan B. Lazrek , Synthesis, characterization, molecular docking, and anticancer activities of new 1,3,4-oxadiazole-5-fluorocytosine hybrid derivatives, *Journal of Molecular Structure* (2022), doi: https://doi.org/10.1016/j.molstruc.2022.134135

Highlights

- 1,3,4-Oxadiazole-5-fluorocytosine hybrids were synthesized and evaluated for their anticancer activity against 4 cancer cell lines.
- Compound **5e** exhibited the best antiproliferative activities against HT-1080 cells.
- Compound **5e** induced apoptosis by activation of caspase 3/7 and arrested cell cycle.
- Molecular docking suggested that compound **5e** activates caspase-3.
- Hybrid compounds showed no detectable anti-SARS-CoV-2 activities.

Synthesis, characterization, molecular docking, and anticancer activities of new 1,3,4-oxadiazole-5-fluorocytosine hybrid derivatives

Az-eddine El Mansouri[1,2], Saida Lachhab[1], Ali Oubella[3], Mehdi Ahmad[5], Johan Neyts[6], Dirk Jochmans[6], Winston Chiu[6]; Laura Vangeel[6]; Steven De Jonghe[6]; Hamid Morjani[7], Mustapha Ait Ali[1], Mohamed Zahouily[2], Yogesh S. Sanghvi[4], Hassan B. Lazrek[1,*]

1 Laboratory of Biomolecular and Medicinal chemistry, Faculty of Science Semlalia, University Cadi Ayyad, Marrakesh, Morocco
2 Laboratoire de Matériaux, Catalyse & Valorisation des Ressources Naturelles, URAC 24, Faculté des Sciences et Techniques, Université Hassan II, Casablanca B.P. 146, 20650, Morocco
3 Laboratoire de Synthese Organique et de Physico-Chimie Moleculaire, Departement de Chimie, Faculte´ des Sciences, Semlalia BP 2390, Marrakech 40001, Morocco
4 Rasayan Inc. 2802 Crystal Ridge Road, Encinitas, CA 92024-6615, U.S.A.
5 ICGM, Univ. Montpellier, CNRS, ENSCM, Montpellier, France
6 Rega Institute for Medical Research, KU Leuven, Leuven, Belgium
7 BioSpecT - EA7506 UFR de Pharmacie, Univ-Reims 51, rue Cognacq Jay 51096 Reims cedex, France

Abstract

Analogs of pyrimidine and 1,3,4-oxadiazole are two well established class of molecules proven as potent antiviral and anticancer agents in the pharmaceutical industry. We envisioned designing new molecules where these two heterocycles were conjugated with the goal of enhancing biological activity. In this vein, we synthesized a series of novel pyrimidine-1,3,4-oxadiazole conjugated hybrid molecules as potential anticancer and antiviral agents. Herein, we present a new design for 5-fluorocytosine-1,3,4-oxadiazole hybrids (**5a**-**h**) connected via a methylene bridge. An efficient synthesis of new derivatives was established, and all compounds were fully characterized by NMR and MS. Eight compounds were evaluated for their cytotoxic activity against fibrosarcoma (HT-1080), breast (MCF-7 and MDA-MB-231), lung carcinoma (A-549), and for their antiviral activity against SARS-CoV-2. Among all compounds tested, the compound **5e** showed marked growth inhibition against all cell lines tested, particularly in HT-1080, with IC_{50} values of 19.56 µM. Meanwhile, all tested compounds showed no anti-SARS-CoV-2 activity, with EC_{50} >100 µM. The mechanism of cell death was investigated using Annexin V staining, caspase-3/7 activity, and analysis of cell cycle progression. The compound **5e** induced apoptosis by the activation of caspase-3/7 and cell-cycle arrest in HT-1080 and A-549 cells at the G2M phase. The molecular docking suggested that the compound **5e** activated caspase-3 via the formation of a stable complex protein-ligand.

Key words: 5-fluorocytosine, 1,3,4-oxadiazole hybrid, cytotoxic activity, apoptosis induction, anti- SARS-CoV-2, molecular docking.

Introduction

Search for the treatment of cancer and viral disease remains one of modern medicine's most difficult challenges. Cancer is the second leading cause of death after heart disease, accounting for one in every eight deaths worldwide [1]. Because of undesirable side effects, drug resistance, and reduced bioavailability of currently available therapeutics, the discovery of new anticancer and antiviral compounds remains a critical component in chemotherapy [2]. Apoptosis (programmed cell death) is a fundamental biological process that allows tumor cells and pathogen-infected cells to be killed and removed efficiently [3]. The sequential activation of a family of cysteinyl-aspartate-specific proteases (Caspases) mediates the apoptosis process [4]. Caspases-3 and -7 are critical effector enzymes in the execution of apoptosis [5]. As a result, apoptosis has emerged as an appealing target for the development of new anticancer agents [6].

Pyrimidine derivatives have a rich history in the field of medicinal chemistry, especially anticancer and antiviral treatment [7-12]. Moreover, being a building-block of DNA and RNA, pyrimidine derivatives were found to be associated with a variety of chemotherapeutic effects including antimicrobial [13], antitubercular [14], antifungal [15], and antimalarial [16] activities. Capecitabine **I** is an anticancer drug containing 5-fluorocytosine pyrimidine base which is an efficient inhibitor of colon cancer cell line HCT-15 through the mitochondrial pathway of apoptosis [17]. Additionally, capecitabine is known to induce apoptosis through the activation of caspase-3 in colorectal cancer caco-2 cell lines [18]. Furthermore, dideoxy-2′-fluoro-4′-thionucleosides 5-fluorocytosine **II** exhibited potent anti-HIV activity with an EC_{50} of 0.15 μM [19]. The carbocyclic nucleoside of 5-fluorocytosine and cytosine **III** showed high selectivity against Venezuela equine encephalitis virus (VEEV) and various strains of H5N1 influenza [20].

1,3,4-Oxadiazole is another useful scaffold in medicinal chemistry offering both versatility and structural diversity for the design of drug molecules. In some cases, it serves as a bioisostere for carbonyl-containing compounds like esters, amides, and carbamates, or as a flat aromatic linker to provide the molecular geometry. Stability of the oxadiazole ring and its ability to interact with bio-targets via $\pi - \pi$ interaction and strong hydrogen bonding justifies our interest in developing bioactive molecules containing this scaffold [21-24]. Stecoza and

coworkers have synthesized a series of new 2,5-diaryl/heteroaryl-1,3,4-oxadiazoles **IV**, which showed promising cytotoxicity against HT-29 (colon adenocarcinoma) and MDA-MB-231 (breast adenocarcinoma). 1,3,4-Oxadiazole compounds **IV** were able to arrest the cell cycle and induced apoptosis in the MDA-MB-231 cell lines [25]. Additionally, a series of new derivatives bearing 1,3,4-oxadiazole moiety **V** were designed, synthesized, and evaluated for their anticancer activities in four human cancer cell lines (HepG2, A549, MCF-7, and HCT-116). These compounds exhibited significant cytotoxic activity with mitochondrial-mediated apoptosis by decreasing mitochondrial membrane potential, up-regulation of Bax, down-regulation of Bcl-2 and activation levels of the caspase cascade [26]. Cancer patients are particularly vulnerable to coronavirus (COVID-19) [27, 28]. These individuals are not only more susceptible to this infection, but also more frequently develop severe pneumonia during the course of disease [29]. However, limited information is known about the outcome of chemotherapy for cancer patients with prior COVID-19 infection [30]. Meanwhile, Rabie *et al*. reported that the oxadiazole **VI** and **VII** exhibited significant anti-COVID-19 activity (anti-SARS-CoV-2 EC_{50} = 0.31 and 1.01 μM, respectively), which could be promising lead compound for the design of new anti-COVID-19 agents [31]. They also proposed two new 1,3,4-oxadiazole compounds CoViTris2020 and ChloViD2020 as the first multitarget coronaviral protein blockers with high potency [32].

Recently, we have synthesized several novel pyrimidine-1,3,4-oxadiazole hybrids with potential anticancer and antiviral agents [33-36]. Continuing our effort to discover bioactive compounds, herein, we report the design and synthesis of new 5-fluorocytosine-1,3,4-oxadiazole hybrids (**5a-h**) conjugated through a methylene bridge. The prepared products were evaluated for their anticancer activities in HT-1080, A-549, MCF-7, and MDA-MB-231 cell lines. We studied the possible mechanism of apoptosis induction mechanism and the activation of caspase-3/7. Molecular docking study was carried out to investigate the ability of compound **5e** to activate the caspase-3 protein. Finally, all compounds (**5a-h)** were tested against anti-COVID-19 activity against Beta Cov / Belgium / GHB-03021/2020.

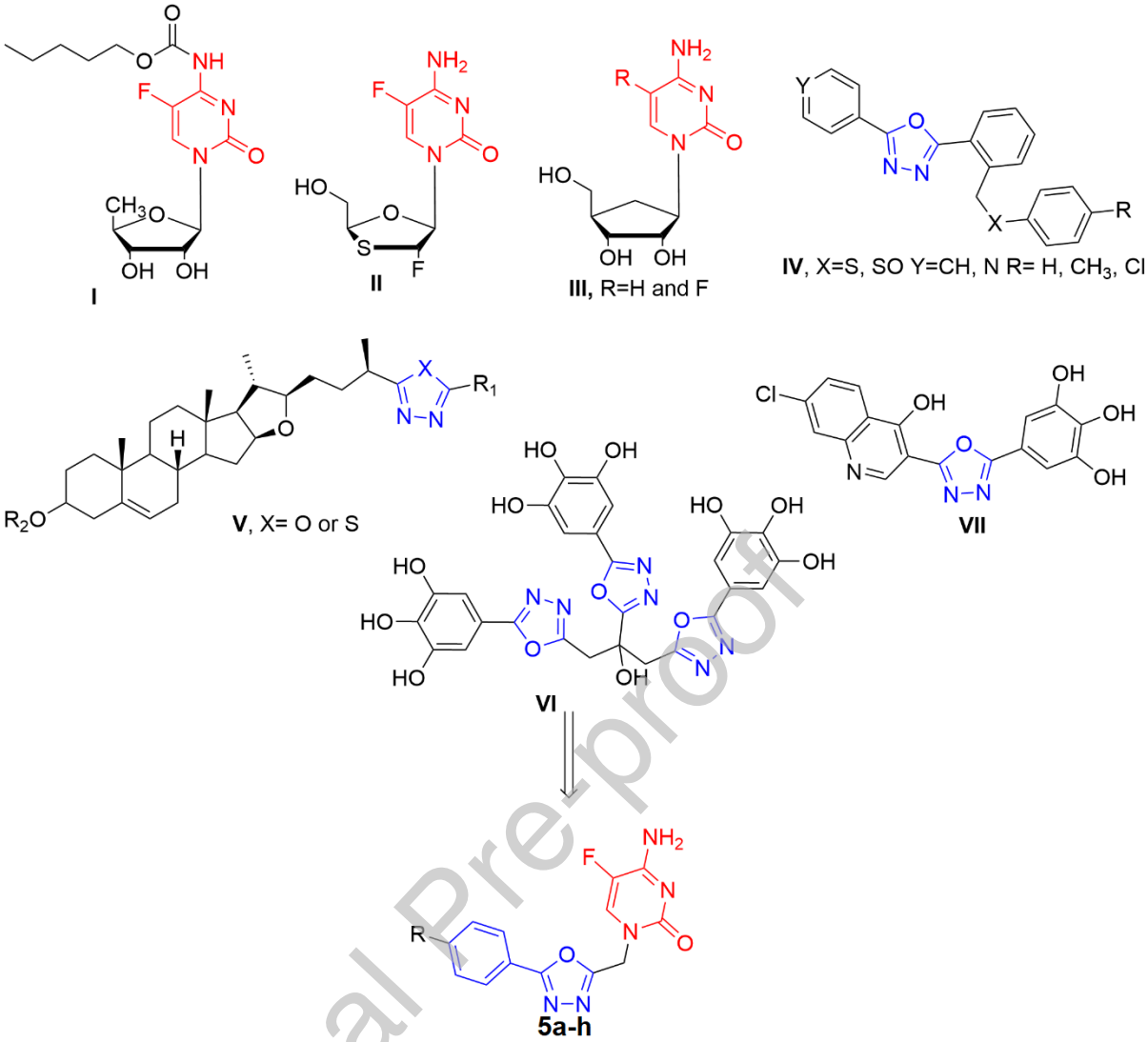

Figure 1: Design of the new 1,3,4-oxadiazole-5-fluorocytosine hybrid derivatives

Materials & Methods

Chemistry

General

Melting points were measured using a Büchi B-545 digital capillary melting point apparatus and used without correction. Reactions were checked with TLC using aluminum sheets with silica gel 60 F254 from Merck. IR Spectra were recorded on a Perkin-Elmer VERTEX 70 FTIR spectrometer covering field 400-4000 cm^{-1}. The ^{1}H NMR and ^{13}C NMR spectra were recorded in DMSO-d_6 or $CDCl_3$ on a Bruker Advance 300 spectrometer at 300 and 75 MHz, respectively. The chemical shifts are expressed in parts per million (ppm) by using DMSO-d_6 as internal reference. The multiplicities of the signals are indicated by the following abbreviations: s, singlet; d, doublet; t, triplet; q, quadruplet; and m, multiplet, and

coupling constants *J* are expressed in Hertz. Mass spectra were collected using an API 3200 LC/MS/MS system, equipped with an ESI source. The chemical reagents used in synthesis were purchased from Fluka, Sigma and Aldrich.

Preparation of alkylating agent 4a-j

First, 10 mmol of individual carboxylic acid **1a-g** was taken in 15 ml of methanol, and thionyl chloride was added dropwise over 10 min at 0 °C. Then, the mixture was stirred at room temperature for 3 hours, methanol was evaporated under vacuum, extracted with ethyl acetate, and purified by column chromatography to afford esters **2a-g**. In the second step, to a round bottom flask (25 mL) equipped with a condenser, individual ester **2a–g** (10 mmol), hydrazine hydrate (11 mmol, 0.5 ml) and ethanol (5 ml) were added. The mixture was refluxed for 3 hours. The solvent was evaporated under vacuum and the hydrazide was recrystallized using ethanol to afford the desired product **3a-g**. Then, chloroacetic acid (11 mmol, 1.04 g), phosphorus oxychloride (30 mmol, 2.8 ml) and DCE (20 ml) were mixed in 100 ml round bottom flask and heated at 80 °C for 2 hours. Next, each carboxylic acid hydrazide (**2a-g**) was added to the mixture and heated for 12 hours. After completion of the reaction, water (40 ml) was added, and the pH was adjusted to 7–8 with sodium hydrogen carbonate and extracted with dichloromethane. The organic layer was dried (Na_2SO_4), evaporated, and purified by column chromatography (silica gel, 5% EtOAc in hexane) to give alkylating agents **4a-g**.

The alkylating agents **4h-j** were prepared by similar procedure. The only difference is the products **1h-i** (10 mmol) were subjected to the benzylation reaction. This reaction was carried out using 11 mmol of benzyl and 4-fluorobenzyl chloride, 10 mmol of potassium carbonate, and 20 ml of acetone at reflux for 12 hours. Compounds **4h-j** were purified by column chromatography using mixture of hexane and ethyl acetate.

*2-(Chloromethyl)-5-phenyl-1,3,4-oxadiazole **(4a)***

Rf = 0.4 (9/1 (Hexane/AcOEt)). IR U (KBr, cm^{-1}): 3029 (Csp2), 2972 (Csp3), 1552 (C=N), 1017 (C-O-C), 746 (C-Cl). ^{1}H NMR (*300 MHz,* $CDCl_3$) δ (ppm): 5.16 (s, 2H, CH_2); 7.6 (m, 3H, H_{Ph}); 8.03 (m, 2H, H_{Ph}). ^{13}C NMR (*75 MHz*, $CDCl_3$) δ (ppm): 33.23 (CH_2); 122.85 ($C_{Ph,IV}$); 126.65 ($C_{Ph,III);}$ 129.53 ($C_{Ph,III);}$132.38 ($C_{Ph,III}$);162.88, 164.95 (Coxa, Coxa).

*2-(Chloromethyl)-5-(2-chlorophenyl)-1,3,4-oxadiazole **(4b)***

Rf = 0.35 (9/1 (Hexane/AcOEt)). IR U (KBr, cm^{-1}): 3018 (Csp2), 2964 (Csp3), 1554 (C=N), 1013 (C-O-C), 753 (C-Cl). ^{1}H NMR (*300 MHz,* $CDCl_3$) δ(ppm): 5.22 (s, 2H, CH_2); 7.5 (d,

$^{3}J_{H-H}$ = 7.2 Hz, 1H, H_{Ph}); 7.62 (d.d, $^{3}J_{H-H}$ = 7.5 Hz et $^{3}J_{H-H}$ = 7.2 Hz, 1H, H_{Ph}); 7.69 (d.d ,$^{3}J_{H-H}$ = 7.5 Hz et $^{3}J_{H-H}$ = 7.2 Hz, 1H, H_{Ph}); 7.93 (d, $^{3}J_{H-H}$ = 7.5 Hz, 1H, H_{Ph}). ^{13}C NMR (*75 MHz*, $CDCl_3$) δ (ppm):35.41 (CH_2); 122.65 ($C_{Ph,IV}$); 127.82 ($C_{Ph,III);}$ 131.52 ($C_{Ph,III}$);131.83 ($C_{Ph,III}$); 132.37 ($C_{Ph,III}$); 133.98 ($C_{Ph,IV}$);162.35, 164.22 (Coxa, Coxa).

2-(Chloromethyl)-5-(3-chlorophenyl)-1,3,4-oxadiazole ***(4c)***

Rf = 0.37 (9/1 (Hexane/AcOEt)). IR U (KBr, cm^{-1}): 3015 (Csp2), 2968 (Csp3), 1562 (C=N), 1021 (C-O-C), 758 (C-Cl). ^{1}H NMR (*300 MHz*, $CDCl_3$) δ (ppm): 5.19 (s, 2H, CH_2); 7.63 (m, 2H, H_{Ph}); 7.92 (m, 2H, H_{Ph}). ^{13}C NMR (*75 MHz*, $CDCl_3$) δ (ppm): 37.52 (CH_2); 124.84 ($C_{Ph,IV}$); 125.14 ($C_{Ph,III);}$ 125.89 ($C_{Ph,III}$);131.62 ($C_{Ph,III}$); 132.02 ($C_{Ph,III}$); 133.17 ($C_{Ph,IV}$);162.53, 164.47 (Coxa, Coxa).

2-(Chloromethyl)-5-(3-nitrophenyl)-1,3,4-oxadiazole ***(4d)***

Rf= 0.22 (9/1 (Hexane/AcOEt)). IR U (KBr, cm^{-1}): 3012 (Csp2), 2972 (Csp3), 1589 (NO_2), 1574 (C=N), 1028 (C-O-C), 755 (C-Cl). ^{1}H NMR (*300 MHz*, $CDCl_3$) δ (ppm): 5.19 (s, 2H, CH_2); 7.63 (t, $^{3}J_{H-H}$ = 7.8 Hz, 1H, H_{Ph}); 8.45 (m, 2H, H_{Ph}); 8.92 (t, $^{4}J_{H-H}$ = 1.8 Hz, 1H, H_{Ph}). ^{13}C NMR (*75 MHz*, $CDCl_3$) δ (ppm): 32.79 (CH_2); 122.06 ($C_{Ph,III}$); 125.00 ($C_{Ph,IV);}$ 126.61 ($C_{Ph,III}$); 130.56 ($C_{Ph,III}$); 132.60 ($C_{Ph,III}$); 162.95, 164.12 (Coxa, Coxa).

2-(Chloromethyl)-5-(4-chlorophenyl)-1,3,4-oxadiazole ***(4e)***

Rf = 0.34 (9/1 (Hexane/AcOEt)). IR U (KBr, cm^{-1}): 3021 (Csp2), 2964 (Csp3), 1568 (C=N), 1011 (C-O-C), 756 (C-Cl). ^{1}H NMR (*300 MHz*, $CDCl_3$) δ (ppm): 5.15 (s, 2H, CH_2); 7.66 (t, $^{3}J_{H-H}$ = 7.5 Hz, 2H, H_{Ph}); 8.01 (d, $^{3}J_{H-H}$ = 7.5 Hz, 2H, H_{Ph}). ^{13}C NMR (*75 MHz*, $CDCl_3$) δ (ppm): 36.23 (CH_2); 121.09 ($C_{Ph,IV}$); 124.62 ($C_{Ph,III);}$ 125.37 ($C_{Ph,III}$);136.45 ($C_{Ph,IV}$); 162.28, 164.12 (C-2, C-3).

2-(Chloromethyl)-5-(4-fluorophenyl)-1,3,4-oxadiazole ***(4f)***

Rf = 0.31 (9/1 (Hexane/AcOEt)). IR U (KBr, cm^{-1}): 3014 (Csp2), 2961 (Csp3), 1584 (C=N), 1079 (C-O-C), 1003 (C-F), 760 (C-Cl). ^{1}H NMR (*300 MHz*, $CDCl_3$) δ (ppm): 4.79 (s, 2H, CH_2); 7.25 (m, 2H, H_{Ph}); 8.12 (m, 2H, H_{Ph}). ^{13}C NMR (*75 MHz*, $CDCl_3$) δ (ppm): 32.96 (CH_2); 116.50 (d, $^{2}J_{C-F}$ = 22 Hz, $C_{Ph,III}$); 119.68 (d, $^{4}J_{C-F}$ = 3 Hz, $C_{Ph,IV}$); 129.47 (d, $^{3}J_{C-F}$ = 9 Hz, $C_{Ph,III}$); 163.72 (d, $^{1}J_{C-F}$ = 228 Hz, $C_{Ph,IV}$); 163.40 , 166.77 (Coxa, Coxa).

2-(Chloromethyl)-5-(4-methylphenyl)-1,3,4-oxadiazole ***(4g)***

Rf = 0.46 (9/1 (Hexane/AcOEt)). IR U (KBr, cm^{-1}): 3020 (Csp2), 2965 (Csp3), 1562 (C=N), 1018 (C-O-C), 760 (C-Cl). ^{1}H NMR (*300 MHz*, $CDCl_3$) δ (ppm): 2.49 (s, 3H, CH_2); 5.58 (s,

2H, H-1); 7.39 (d, $^{3}J_{H\text{-}H}$ = 8.1 Hz, 2H, H_{Ph}); 7.82 (d, $^{3}J_{H\text{-}H}$ = 8.1 Hz, 2H, H_{Ph}). ^{13}C NMR (*75 MHz*, $CDCl_3$) δ (ppm): 21.64 (CH_3); 39.12 (CH_2); 115.04 ($C_{Ph,IV}$); 126.87 ($C_{Ph,III}$); 130.50 ($C_{Ph,III}$); 132.85 ($C_{Ph,IV}$); 162.81, 164.77 (Coxa, Coxa).

*2-(Chloromethyl)-5-(4-((4-fluorobenzyl)oxy)phenyl)-1,3,4-oxadiazole (**4h**)*

Rf = 0.39 (9/1 (Hexane/AcOEt)). IR U (KBr, cm^{-1}): 3078 (Csp2), 2986 (Csp3),1563 (C=N),1018 (C-O-C), 760 (C-Cl). ^{1}H NMR (*300 MHz*, DMSO-*d*6) δ (ppm): 5.19 (s, 2H, CH_2); 5.61 (s, 2H, CH_2); 7.18 (d, ^{3}J = 8.7 Hz, 4H, H_{Ph}); 7.55 (d,^{3}J = 6.6 Hz, 2H, $2H_{Ph}$); 7.93 (d, 2H, $2H_{Ph}$). ^{13}C NMR (*75 MHz*, DMSO-*d6*) δ(ppm): 22.08 (CH_2); 69.02 (CH_2); 115.42 (d, $^{2}J_{C\text{-}F}$ = 21 Hz, $C_{Ph,III}$); 115.69 ($C_{Ph,III}$); 115.81 ($C_{Ph,III}$); 128.30 ($C_{Ph,IV}$); 132.56 (d, $^{4}J_{C\text{-}F}$ = 3 Hz, $C_{Ph,III}$); 159.85 ($C_{Ph,IV}$-O); 162.51 (d, $^{1}J_{C\text{-}F}$ = 225 Hz, $C_{Ph,IV}$-F); 162.78, 164.52 (Coxa, Coxa).

Synthesis of homonucleosides (5a-h)

A mixture of 5-fluorocytosine (1 mmol), alkylating agent (0.75 mmol) and potassium carbonate (0.5 mmol) in DMF (10 ml) were heated at 60 ° C for 2 hours. The solvent was evaporated, and residue was purified by column chromatography with CH_2Cl_2 / MeOH (95/5) to obtain pure products (**5a-h**).

*4-Amino-5-fluoro-1-((5-phenyl-1,3,4-oxadiazol-2-yl)methyl)pyrimidin-2(1H)-one (**5a**)*

Rf = 0.43 (9/1 (CH_2Cl_2/MeOH)). Mp (°C) 267–269. IR U (KBr, cm^{-1}): 3348 (NH); 3070 (Csp2); 1687(C=O); 1640 (C=O); 1138 (C-F). ^{1}H NMR (*300 MHz*, DMSO-*d*6) δ (ppm): 5.17 (s, 2H, CH_2); 7.57 (m, 4H, NH + $3H_{Ph}$); 7.90 (s, 1H, NH); 7.98 (m, 2H, 2 H_{Ph}); 8.15 (d, $^{3}J_{H\text{-}F}$ = 6.6 Hz, 1H, H-6). ^{13}C NMR (*75 MHz*, DMSO-*d6*) δ(ppm): 43.39 (CH_2); 123.05 ($C_{Ph,IV}$); 126.47 ($C_{Ph,III}$); 126.47 ($C_{Ph,IV}$);129.48 ($C_{Ph,III}$); 130.36 (d, $^{2}J_{C\text{-}F}$ = 39 Hz, C-6); 135.72 (d, $^{1}J_{C\text{-}F}$ = 240 Hz, C-5); 153.74 (C-2); 158.07 (d, $^{2}J_{C\text{-}F}$ = 13 Hz, C-4); 163.10, 164.14 (Coxa, Coxa). HRMS for $C_{13}H_{11}FN_5O_2^+$ calculated 288.0891, found 288.0891.

*4-Amino-1-((5-(2-chlorophenyl)-1,3,4-oxadiazol-2-yl)methyl)-5-fluoropyrimidin-2(1H)-one (**5b**)*

Rf = 0.45 (9/1 (CH_2Cl_2/MeOH)). Mp (°C) 242–244. IR U (KBr, cm^{-1}): 3348 (NH); 3069 (Csp2); 1687 (C=O); 1642 (C=O); 1139 (C-F); 743 (C-Cl). ^{1}H NMR (*300 MHz*, DMSO-*d*6) δ(ppm): 5.20 (s, 2H, CH_2); 7.57 (t, $^{3}J_{H\text{-}H}$ = 7.2 Hz,1H, H_{Ph}); 7.62 (m, 3H, 2 H_{Ph} + NH); 7.90 (s, 1H, NH); 7.94 (d.d, $^{3}J_{H\text{-}H}$ = 7.8 Hz et $^{3}J_{H\text{-}H}$ = 7.5 Hz, 1H, H_{Ph}); 8.14 (d, $^{3}J_{H\text{-}F}$ = 6.6 Hz,1H, H-6). ^{13}C NMR (*75 MHz*, DMSO-*d6*) δ(ppm): 43.39 (CH_2);122.24 ($C_{Ph,IV}$); 127.1 ($C_{Ph,III}$); 130.12 ($C_{Ph,IV}$); 130.54 ($C_{Ph,III}$); 131.13 ($C_{Ph,III}$); 131.46 (d, $^{2}J_{C\text{-}F}$ = 39 Hz, C-6); 133.32

($C_{Ph,III}$);135.84 (d, $^{1}J_{C-F}$ = 240 Hz, C-5); 153.75 (C-2); 158.08 (d, $^{2}J_{C-F}$ = 13 Hz, C-4); 162.28, 163.48 (Coxa, Coxa). HRMS for $C_{13}H_{10}ClFN_5O_2^+$ calculated 322.0502, found 322.0506.

4-Amino-1-((5-(3-chlorophenyl)-1,3,4-oxadiazol-2-yl)methyl)-5-fluoropyrimidin-2(1H)-one ***(5c)***

Rf = 0.44 (9/1 (CH_2Cl_2/MeOH)). Mp (°C) 264–266. ^{1}H NMR (*300 MHz*, DMSO-*d*6) δ (ppm): 5.18 (s, 2H, CH_2); 7.66 (m,3H, 2H_{Ph} + NH); 7.89 (s, 1H, NH); 7.94 (m, 2H, H_{Ph}); 8.14 (d, $^{3}J_{H-F}$ = 6.9 Hz,1H, H-6). ^{13}C NMR (*75 MHz*, DMSO-*d6*) δ(ppm): 43.34 (CH_2); 124.97 ($C_{Ph,IV}$); 125.20 ($C_{Ph,III}$); 125.94 ($C_{Ph,III}$); 130.33 (d, $^{2}J_{C-F}$ = 31 Hz, C-6); 131.53 ($C_{Ph,III}$); 131.92 ($C_{Ph,III}$); 134.06 ($C_{Ph,IV}$); 135.85 (d, $^{1}J_{C-F}$ = 240 Hz, C-5); 153.73 (C-2); 158.08 (d, $^{2}J_{C-F}$ = 13 Hz, C-4);163.05, 163.46 (Coxa, Coxa).IR U (KBr, cm^{-1}): 3068 (Csp2); 1688 (C=O);1640 (C=O); 1140 (C-F); 743 (C-Cl). HRMS for $C_{13}H_{10}ClFN_5O_2^+$ calculated 322.0502, found 322.0510.

4-Amino-1-((5-(3-nitrophenyl)-1,3,4-oxadiazol-2-yl)methyl)-5-fluoropyrimidin-2(1H)-one ***(5d)***

Rf = 0.41 (9/1 (CH_2Cl_2/MeOH)). Mp (°C) 251–253. ^{1}H NMR (*300 MHz*, DMSO-*d*6) δ (ppm): 5.22 (s, 2H, CH_2); 7.66 (s, 1H, NH); 7.90 (m, 2H, H_{Ph} + NH);8.16 (d, $^{3}J_{H-F}$ = 6.6 Hz,1H, H-6); 8.40 (d.t, $^{3}J_{H-H}$ = 7.8 Hz et $^{4}J_{H-H}$ = 1.2 Hz, 1H, H_{Ph}); 8.47 (m, 1H, H_{Ph}). ^{13}C NMR (*75 MHz*, DMSO-*d6*) δ(ppm): 43.35 (CH_2);120.99 ($C_{Ph,IV}$); 124.49 ($C_{Ph,IV}$); 126.45 ($C_{Ph,III}$);130.33 (d, $^{2}J_{C-F}$ = 32 Hz, C-6);131.42 ($C_{Ph,III}$); 132.55 ($C_{Ph,III}$);135.86 (d, $^{1}J_{C-F}$ = 240 Hz, C-5);148.21 ($C_{Ph,IV}$); 153.74 (C-2); 158.09 (d, $^{2}J_{C-F}$ = 13 Hz, C-4);162.7, 163.79 (Coxa, Coxa).IR U (KBr, cm^{-1}): 3347 (NH); 3069 (Csp2); 1686 (C=O); 1641 (C=O); 1573 (N-O); 1139 (C-F); HRMS for $C_{13}H_{10}FN_6O_4^+$ calculated 333.0742, found 333.0732.

4-Amino-1-((5-(4-chlorophenyl)-1,3,4-oxadiazol-2-yl)methyl)-5-fluoropyrimidin-2(1H)-one ***(5e)***

Rf = 0.43 (9/1 (CH_2Cl_2/MeOH)). Mp (°C) 317–319. ^{1}H NMR (*300 MHz*, DMSO-*d*6) δ (ppm): 5.17 (s, 2H, CH_2); 7.67 (m, 3H, 2H_{Ph} + NH); 7.89 (s, 1H, NH); 7.97 (d, $^{3}J_{H-H}$ = 8.4 Hz, 2H, H_{Ph}); 8.13 (d, $^{3}J_{H-F}$ = 6.9 Hz, 1H, H-6). ^{13}C NMR (*75 MHz*, DMSO-*d6*) δ (ppm): 43.37 (CH_2);121.93 ($C_{Ph,IV}$); 128.29 ($C_{Ph,III}$); 129.65 ($C_{Ph,III}$);130.33 (d, $^{2}J_{C-F}$ = 31 Hz, C-6); 135.83 (d, $^{1}J_{C-F}$ = 240 Hz, C-5); 136.80 ($C_{Ph,IV}$); 153.73 (C-2); 158.08 (d, $^{2}J_{C-F}$ = 13 Hz, C-4); 163.27, 163.41 (Coxa, Coxa). IR U (KBr, cm^{-1}): 3348 (NH); 3069 (Csp2); 1686(C=O); 1640(C=O); 1140 (C-F); 744 (C-Cl). HRMS for $C_{13}H_{10}ClFN_5O_2^+$ calculated 322.0502, found 322.0502.

*4-Amino-1-((5-(4-toluyl)-1,3,4-oxadiazol-2-yl)methyl)-5-fluoropyrimidin-2(1H)-one (****5f****)*

Rf = 0.17 (9.5/0.5 (CH_2Cl_2/MeOH)). Mp (°C) 271–273. ^{1}H NMR (*300 MHz*, DMSO-*d*6) δ (ppm): 2.39 (CH_3); 5.16 (s, 2H, CH_2); 7.41 (d, 2H, $2H_{Ph}$); 7.65 (s, 1H, NH); 7.97 (m, 3H, NH + $2H_{Ph}$); 8.14 (d, $^3J_{H\text{-}F}$ = 6.9 Hz, 1H, H-6). ^{13}C NMR (*75 MHz*, DMSO-*d6*) δ (ppm): 43.39(CH_2); 123.05 ($C_{Ph,IV}$); 126.47 ($C_{Ph,III}$); 129.48 ($C_{Ph,III}$); 130.64 (d, $^2J_{C\text{-}F}$ = 31 Hz, C-6); 132.08 ($C_{Ph,IV}$); 135.85 (d, $^1J_{C\text{-}F}$ = 240 Hz, C-5); 153.74 (C-2); 158.13 (d, $^2J_{C\text{-}F}$ = 13 Hz, C-4); 163.10, 163.14 (Coxa, Coxa).IR U (KBr, cm^{-1}): 3348 (NH); 3067 (Csp^2); 1686 (C=O);1639 (C=O); 1184 (C-F); HRMS for $C_{14}H_{13}FN_5O_2^+$ calculated 302.1048, found 302.1044.

*4-Amino-1-((5-(4-fluorophenyl)-1,3,4-oxadiazol-2-yl)methyl)-5-fluoropyrimidin-2(1H)-one (**5g**)*

Rf = 0.40 (9/1 (CH_2Cl_2/MeOH)). Mp (°C) 293–295. ^{1}H NMR (*300 MHz*, DMSO-*d*6) δ (ppm):5.17 (s, 2H, CH_2); 7.45 (t, ^3J = 7.2 Hz, 2H, $2H_{Ph}$); 7.65 (s, 1H, NH); 7.88 (s, 1H, NH); 8.03 (m, 2H, H_{Ph}); 8.13 (d, $^3J_{H\text{-}F}$ = 6.6 Hz,1H, H-6). ^{13}C NMR (*75 MHz*, DMSO-*d6*) δ (ppm):43.35 (CH_2);116.73 (d, $^2J_{C\text{-}F}$ = 22 Hz, $C_{Ph,III}$); 119.74 (d, $^4J_{C\text{-}F}$ = 3 Hz, $C_{Ph,IV}$); 129.22 (d, $^3J_{C\text{-}F}$ = 9.15 Hz, $C_{Ph,III}$);130.33 (d, $^2J_{C\text{-}F}$ = 34 Hz, C-6); 135.83 (d, $^1J_{C\text{-}F}$ = 240 Hz, C-5); 153.73 (C-2); 158.08 (d, $^2J_{C\text{-}F}$ = 13 Hz, C-4);163.11, 163.42 (Coxa, Coxa); 164.11 (d, $^1J_{C\text{-}F}$ = 249 Hz, $C_{Ph,IV}$).IR U (KBr, cm^{-1}): 3349 (NH); 3067 (Csp2); 1684(C=O);1639 (C=O); 1185 (C-F); HRMS for $C_{13}H_{10}F_2N_5O_2^+$ calculated 306.0797, found 306.0799.

*4-Amino-5-fluoro-1-((5-(4-((4-fluorobenzyl)oxy)phenyl)-1,3,4-oxadiazol-2-yl)methyl)pyrimidin -2(1H)-one (**5h**)*

Rf = 0.46 (9/1 (CH_2Cl_2/MeOH)). Mp (°C) 290-292. ^{1}H NMR (*300 MHz*, DMSO-*d*6) δ (ppm): 5.15 (s, 2H, CH_2); 5.18 (s, 2H, CH_2); 7.23 (d, ^3J = 9 Hz, 4H, H_{Ph}); 7.54 (m, 2H, $2H_{Ph}$); 7.65 (s, 1H, NH); 7.90 (m, 3H, $2H_{Ph}$ + NH); 8.14 (d, $^3J_{H\text{-}F}$ = 6.6 Hz,1H, H-6). ^{13}C NMR (*75 MHz*, DMSO-*d6*) δ (ppm): 43.35 (CH_2); 68.78 (CH_2); 115.29 (d, $^2J_{C\text{-}F}$ = 21 Hz, $C_{Ph,III}$); 115.64 ($C_{Ph,III}$); 115.67 ($C_{Ph,III}$); 128.23 ($C_{Ph,IV}$); 130.34 (d, $^2J_{C\text{-}F}$ = 33 Hz, C-6); 132.62 (d, $^4J_{C\text{-}F}$ = 3 Hz, $C_{Ph,III}$); 135.83 (d, $^1J_{C\text{-}F}$ = 240 Hz, C-5); 153.74 (C-2); 158.08 (d, $^2J_{C\text{-}F}$ = 13 Hz, C-4); 160.23 ($C_{Ph,IV}$-O); 162.53 (d, $^1J_{C\text{-}F}$ = 225 Hz, $C_{Ph,IV}$-F); 162.52, 163.46 (Coxa, Coxa). IR U (KBr, cm^{-1}): 3349 (NH); 3067 (Csp^2); 1684 (C=O); 1639 (C=O); 1286 (C-O); 1185 (C-F); 1117 (C-O). HRMS for$C_{20}H_{16}F_2N_5O_3^+$ calculated 412.1216, found 412.1208.

Biology

Anti-SARS-CoV-2

The SARS-CoV-2 isolate used was derived from the BetaCov/Belgium/GHB-03021/2020 (EPI ISL407976|2020-02-03), which was isolated from a Belgian patient returning from Wuhan in February 2020. The isolate was passaged 7 times on VeroE6 cell lines which introduced two series of amino acid deletions in the spike protein [37]. The infectious content of the virus stock was determined by titration on Vero E6 cell lines.

The SARS-CoV-2 antiviral assay is based on the previously established SARS-CoV assay [38]. Upon infection the fluorescence of VeroE6-GFP cell cultures declines due to the cytopathogenic effect of the replicating virus. In the presence of an antiviral compound, the cytopathogenicity is inhibited and the fluorescent signal maintained. To this end VeroE6-GFP cell lines (kindly provided by Marnix Van Loock, Janssen Pharmaceutica, Beerse, Belgium), were used as described previously [39, 40]. Since VeroE6 cell lines show a high efflux of some chemotypes, the antiviral assays were performed in the presence of the P-glycoprotein (Pgp) efflux inhibitor CP-100356 (0.5 μM) [41].

Anticancer activity evaluation

Cell culture

Four cancer cell lines: HT-1080 fibrosarcoma, A-549 lung carcinoma, MCF-7, and MDA-MB-231 breast adenocarcinoma were kindly provided by Dr. P. Coursaget from INSERM (Tours, France). A-549, MCF-7, and MDA-MB-231 cell lines were cultured in DMEM, whereas HT-1080 cell lines were cultured in MEM culture media, both supplemented with 10% (v/v) fetal bovine serum (FBS) and 1% penicillin–streptomycin. The cells were incubated at 37°C in a humidified atmosphere with 5% CO_2.

Cytotoxicity and antiproliferative activity

Cells were seeded in 96-well plates at a density of 5×103 cells/well for 24 hours. Subsequently, cells were treated with various concentrations of the compounds **5a-h** for 24 hours. Doxorubicin (TEVA Pharma S.A., Courbevoie, France) was used as a positive control. Cell growth was analyzed using MTT (3[4,5-dimethylthiazol-2-yl-]2,5-diphenyl tetrazolium bromide) assay. Cells were incubated with 5 mg/mL of MTT for 4h at +37 °C. The supernatant was then discarded before dissolving the product of the reaction formazan with 150μL of DMSO. The absorbance was then measured at 570 nm wavelength using a microplate reader (Thermo Scientific, Paris, France). IC_{50} was estimated using Graph Pad Prism7.

Annexin V binding assay

Cells were seeded at a density of 2×10^5/wells and incubated overnight at 37 °C. The cells were then treated with the compound **5e** at concentration of 20 µM for 24 hours. Cells were then harvested and washed twice with phosphate-buffered saline (PBS) at 4 °C. Cells were centrifuged at 300 g for 5 min and washed twice with PBS at 4 °C before adding 100 µL of Annexin V Binding Buffer staining (Annexin V Apoptosis Detection KIT with 7-AAD, Millipore-Merck, Fontenay sous Bois, France). The cells were incubated for 20 min at room temperature in the dark. Apoptotic cells were evaluated using a Muse Cell Analyzer (Millipore-Merck).

Caspase-3/7 activity

Cells were treated with 20 µM concentration of the compound **5e**. After 24 hours incubation, cells were harvested and washed twice with PBS at 4 °C. After staining with the Caspase assay kit (Promega) and incubation for 30 min, caspase-3 activity was analyzed according to the manufacturer instructions using the Muse Cell Analyzer (Millipore-Merck).

Cell cycle assay

Cells were treated with 20µM of the compound **5e** for 24 hours. The cells were then harvested and washed with PBS. The collected cells (10^6 cells) were suspended into ice-cold ethanol 70% at -20 °C for fixation. After washing, the cells were pelleted by gentle centrifugation and suspended in 1 mL of staining buffer (100 mM Tris, pH = 7.4, 150 mM NaCl, 1mM $CaCl_2$, 0.5 mM $MgCl_2$, 0.1% Nonidet P-40) containing 3 µM propidium iodide (PI) (Millipore-Merck). The cells were then incubated for 15 min at room temperature and analyzed for cell cycle phase distribution using the Muse Cell Analyzer (Millipore-Merck).

Molecular docking

In silico computational docking studies were performed using AutoDock 4.2 [42, 43]. The X-ray crystallographic structure of caspase-3 was downloaded from the RCSB Protein Data Bank (PDB) ID: 6CKZ [44]. The protein was prepared separately by removing water and co-crystalized ligands bound with the protein to make receptor free of any ligand before docking. Polar hydrogen and Gastieger charges were added using the MGL tools and protein saved in PDBQT format. Ligand structure was created separately using ChemDraw Ultra 12.0, energy minimized in Chem3D, torsional bonds of ligands were set flexible and saved in PDBQT format [45]. The receptor was kept rigid and the grid covering all amino acid residues present

inside the active site of protein was built (grid box size of 50 Å x 50 Å x 50 Å with a spacing of 0.375 Å between the grid points and centered at 35.58 (x), 94.397 (y) and 17.54 (z)). The best conformers were searched by the Lamarckian genetic algorithm (LGA), the population size was set to 150 and the maximum number of energy evaluation was set to 25000000. Finally, the results were analyzed and visualized by discovery studio.

Results and discussions

Chemistry

The reaction sequences of the prepared products are summarized in Schemes 1-3. First, the esterification of benzoic acid derivatives **1a-g** was carried out using thionyl chloride and methanol to obtain esters **2a-g** in 87-97% yields. Then, compounds **2a-g** were reacted with hydrazine in ethanol as a solvent to afford hydrazides **3a-g**. Oxadiazoles **4a-g** were synthesized via condensation of hydrazides **3a-g** and chloroacetic acid in the presence of $POCl_3$ and dichloroethane at 80 °C. The 4-fluorobenzyloxy (OCH_2-Ph) has been incorporated in the para position of phenyl ring to synthesize other oxadiazole derivatives (**4a-g**). The 4-hydroxybenzoic acid was esterified with methanol. The obtained product **1h** was subjected to benzylation with 4-fluorobenzyl bromide to form the compound **2h**. The latter was subjected to hydrazinolysis in ethanol to afford the hydrazide **3h**. Finally, we obtained the alkylating agent **4h** by reacting product **3h** and chloroacetic acid in the presence of $POCl_3$.

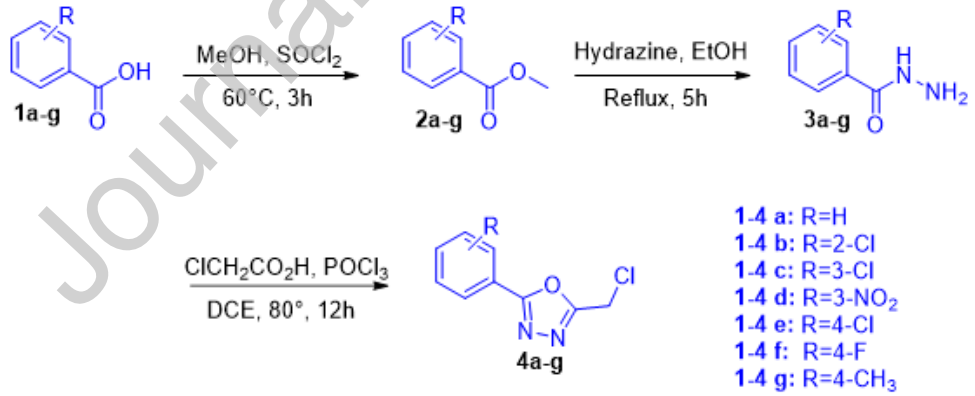

	R	H	2-Cl	3-Cl	3-NO_2	4-Cl	4-F	4-CH_3
Yield (%)	2	94	95	93	87	92	91	93
	3	70	76	71	65	73	79	77
	4	68	70	66	59	68	72	75

*Scheme 1: Synthesis of alkylating agents **4a-g***

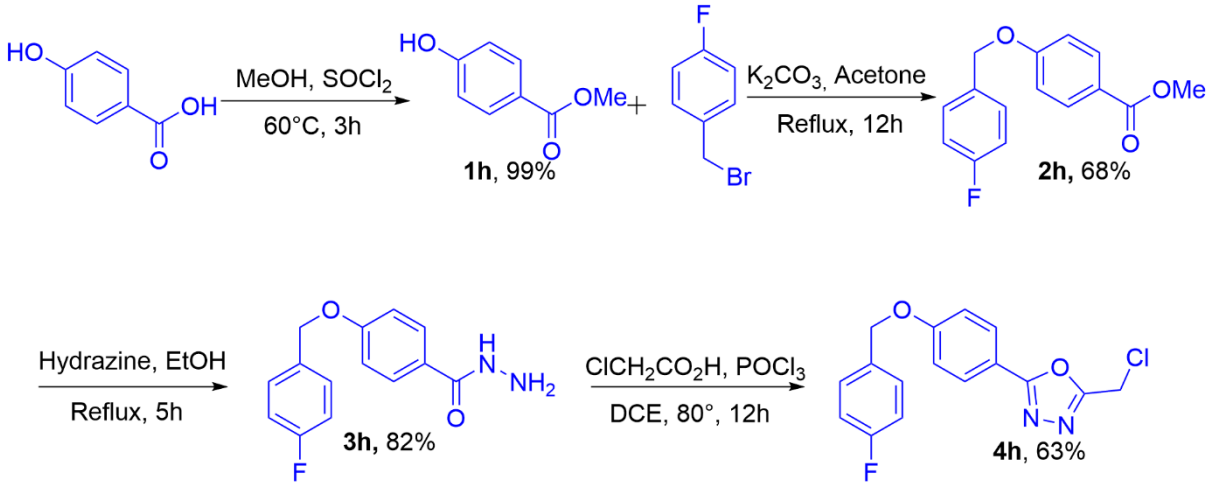

*Scheme 2: Synthesis of alkylating agents **4h***

We used the modified Hilbert–Johnson reaction to synthesize the new 5-fluorocytosine-1,3,4-oxadiazole hybrid conjugates (**5a-h**) [46]. This method afforded the desired product **5a** in a low yield (12%). The reaction yield was improved when a basic medium (K_2CO_3) in dimethylformamide was employed for the conjugation step [45]. The 5-fluorocytosine-1,3,4-oxadiazole derivatives (**5a-h**) were obtained in 45-53% yield. Molecules **5a-h** were fully characterized by ^{1}H NMR, ^{13}C NMR, DEPT, HRMS, and FTIR.

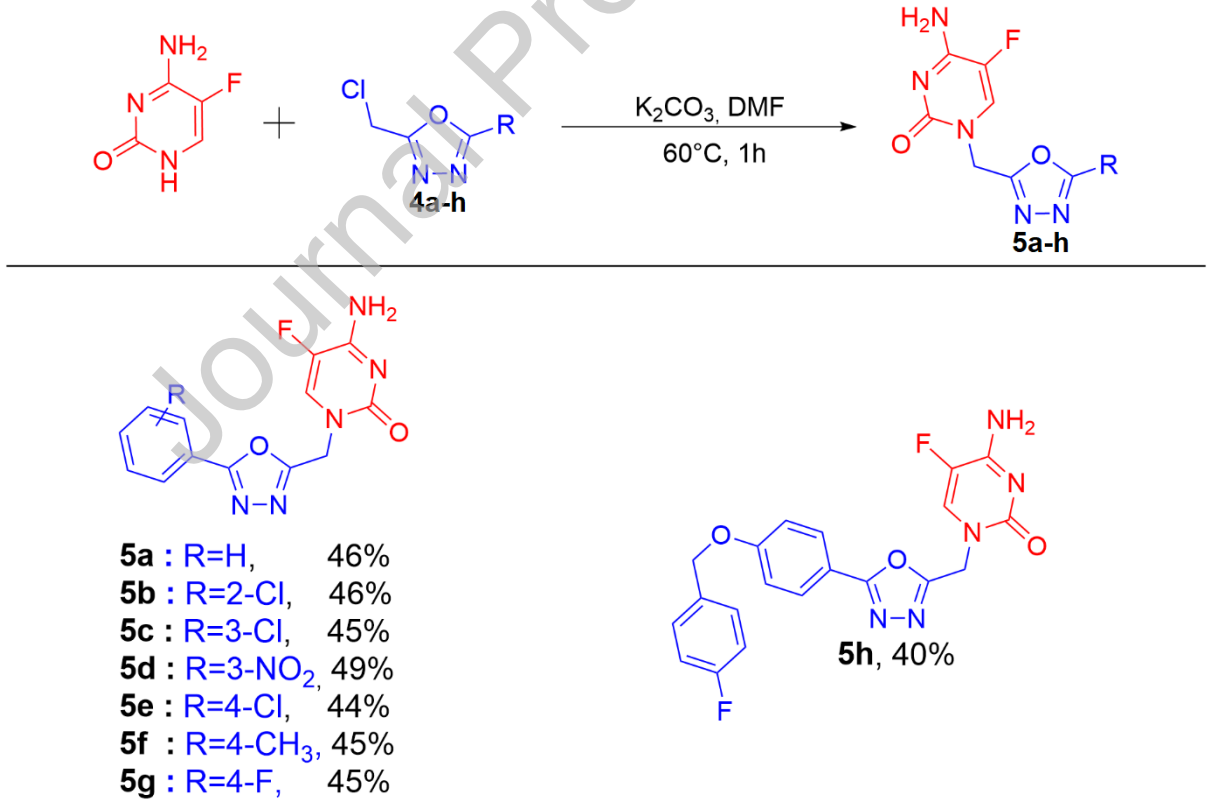

*Scheme 3 : Synthesis of 1,3,4-oxadiazole hybrids **5a-h***

Biology

Anti-proliferative activity

The *in-vitro* antiproliferative activities of hybrids **5a-h** against four human cancer cell lines fibrosarcoma (HT-1080), breast (MCF-7 and MDA-MB-231), and lung carcinoma (A-549) were evaluated by the MTT assay using DOX as a positive control [47-49]. The IC_{50} values are listed in Table 1. Most compounds showed more antiproliferative activity in HT-1080 and A-549 cell lines. The compounds **5e** and **5f** displayed promising antiproliferation properties for both of the above-mentioned cell lines (Table 1). Meanwhile, oxadiazole **5g** containing the fluorine atom at para-position of the phenyl moiety was the most potent against MCF-7 cell lines (21.3 ± 2.18). In MDA-MB-231 lines, the benzyloxy derivative **5h** showed the highest activity in the MDA-MB-231 cell lines, with an IC_{50} value of 21.66 ± 0.95 µM. In summary, compound **5e** was found to be the most potent with IC_{50} of 19.56 ± 1.62 µM and its mechanism of action was studied using molecular docking study.

*Table 1: In-vitro anticancer activity (IC_{50}) of 1,3,4-oxadiazole-5-fluorocytosine hybrids (**8a-i**) against HT1080, A549, MCF7 and MDA-MB231*

Product	IC_{50} (µM)			
	HT-1080	A-549	MCF-7	MDA-MB-231
5a	51.07 ± 5.32	39.41 ± 1.85	42.63 ± 7.11	63.14 ± 4.19
5b	67.14 ± 3.66	46.64 ± 3.05	50.32 ± 1.63	63.73 ± 4.08
5c	50.17 ± 2.42	67.04 ± 6.35	48.43 ± 6.07	58.22 ± 9.46
5d	31.44 ± 1.88	26.9 ± 2.34	21.39 ± 1.50	25.94 ± 2.25
5e	**19.56 ± 1.62**	**20.08 ± 2.83**	27.18 ± 1.95	23.98 ± 4.27
5f	20.87 ± 2.04	27.33 ± 5.91	30.43 ± 3.09	35.31 ± 2.66
5g	37.76 ± 0.25	25.87 ± 3.11	**21.3 ± 2.18**	22.74 ± 2.41
5h	21.88 ± 1.25	25.45 ± 2.04	30.24 ± 2.87	**21.66 ±0.95**
DOX	6.24 ± 0.96	5.30±0.51	4.84±0.31	4.05±0.67

Anti-SARS-CoV-2

SARS-CoV-2 is a positive-sense single-strand RNA virus-like HCV and other flaviviruses [50, 51]. These viruses share a similar replication mechanism requiring an RNA-dependent RNA polymerase (RdRp). Elfiky used a molecular docking study to predict that some nucleosides such as Ribavirin, Remdesivir, Sofosbuvir, Galidesivir, and Tenofovir may have inhibitory activity against SARS-CoV-2 RdRp [52] or non-nucleosides [31, 32]. Significant efforts have been made in both vaccine research for the prevention of COVID-19, as well as

in the identification and utilization of novel or repurposed therapeutics for the management of those with symptomatic COVID-19. To date, eleven agents have received emergency use authorization (EUA) by the US Food and Drug Administration (US FDA) for the management of patients with COVID. This includes two nucleosides as antiviral agents, adenosine nucleoside analog remdesivir and β-D-N^4-hydroxycytidine (NHC, molnupiravir) [53]. In this context, all synthesized homonucleoside analogues (**5a-h**) were evaluated for their anti-SARS-CoV-2 activity against β Cov/Belgium/GHB-03021/2020 in VeroE6 cell lines. All tested compounds showed no anti-SARS-CoV-2 activity, with EC_{50} >100μM. The coronavirus RdRp is a well-established drug target to treat coronavirus infections such as SARS, MERS, and now COVID-19. This polymerase shares similar catalytic mechanisms and displays active site conservation among different positive-sense RNA viruses, including coronaviruses [54]. Moreover, nucleotide analogues that inhibit polymerases are an important group of antiviral agents [55]. To prevent and slow SARS CoV-2 replication and disease progression, nucleoside analogues has been used. For instance, remdesivir and molnupiravir has been used to treat COVID-19. Remdesivir, a phosphoramidate prodrug, is converted into an adenosine triphosphate analogue inside virus-infected cells, which inhibits the RdRps of MERS-CoV, SARS-CoV, and SARS-CoV-2 [56]. It has been also demonstrated that molnupiravir can participate in viral replication and increase G to A and C to U substitution (Base pairing), introducing mutations in viral synthesis and inactivating the progeny viruses [57, 58]. As a result, the lack of activity of our compounds against SARS-CoV-2 can be explained by the fact that synthesized compounds are not recognized by the RdRp enzyme. Moreover, in contrast to molnupiravir and remdesivir the absence of the primary alcohol (which undergoes phosphorylation by the enzymes) in synthesized compounds could be a secondary reason for no activity.

Annexin V7-AAD dual staining analysis

Flow cytometry was carried out using annexin-V/7-AAD dual staining analysis to study the mechanism of cell death [59]. The HT-1080 and A-549 cell lines were treated with 20 μM of oxadiazole derivative **5e** for 24 hours. The data is shown in Figure 2. The early apoptosis percentage increased from 0.06 to 1.02% for HT-1080 and from 1.47 to 11.62% for A-549 cell lines compared to the control. The rate of early apoptosis was enhanced by 17- and 8-fold in HT-10810 and A-549 lines, respectively. The late apoptosis rate was increased from 0.25 to 15.81% in HT-1080 cell lines and from 0.29 to 12.28% in A-549. There was also a significant increase (more than 60-fold) in the levels of total apoptosis in the DOX-treated cancer cell

lines. Thus, this product induces apoptosis, which is characterized by significant positive staining of annexin V.

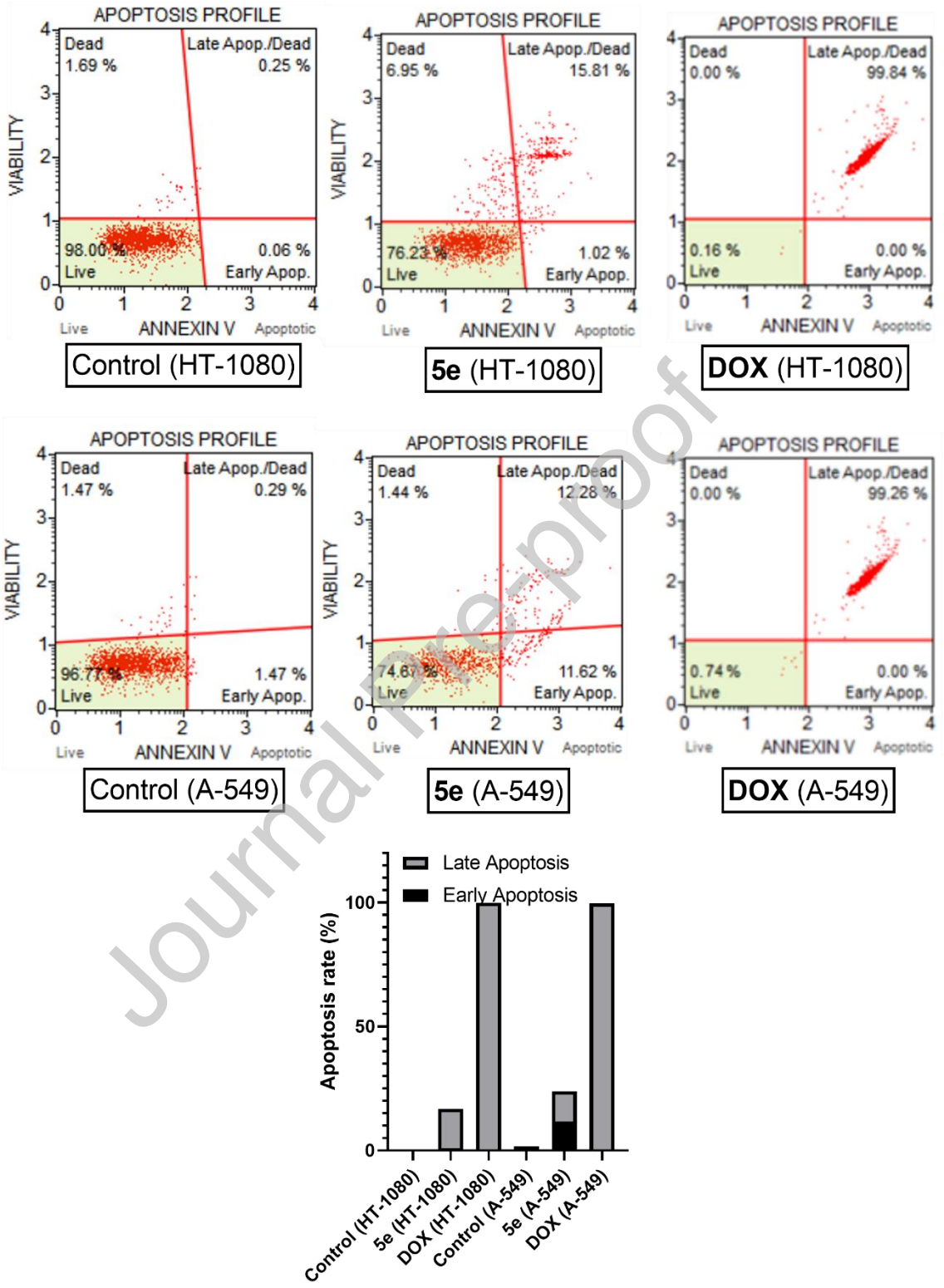

*Figure 2: Annexin V-FITC/7-AAD double staining for detection of apoptosis in HT-1080 and A549 cells after treatment with 20 µM of compound **5e** as well as control (DMSO) for 24 hours. Compound **5e** induces apoptosis.*

Effect of compound 5e on Caspase 3/7 activity

The mechanism of apoptotic induction by the most potent compound **5e** was investigated using caspase 3/7 activation assay in HT-1080 and A-549 cell lines. The proteolytic activity of caspase 3/7 was studied by the effect of compound **5e** at 20μM for 24 hours. As presented in Figure 3, the rate of caspase-3/7 was increased from 6.38 and 4.55 to 19.03 and 16.2 in HT-1080 and A-549 cell lines, respectively. Thus, the percentage of caspase 3/7 was enhanced by 2.54- and 3.6-fold in HT-1080 and A-549 cell lines. On the other hand, there was a significant increase (more than 15-fold) in the levels of caspase-3/7 in DOX-treated cancer cell lines. Accordingly, these results were concordant with that of the flow cytometric analysis of apoptosis and revealed that compound **5e** induced caspase 3/7 activation in fibrosarcoma and adenocarcinoma cancer cell lines.

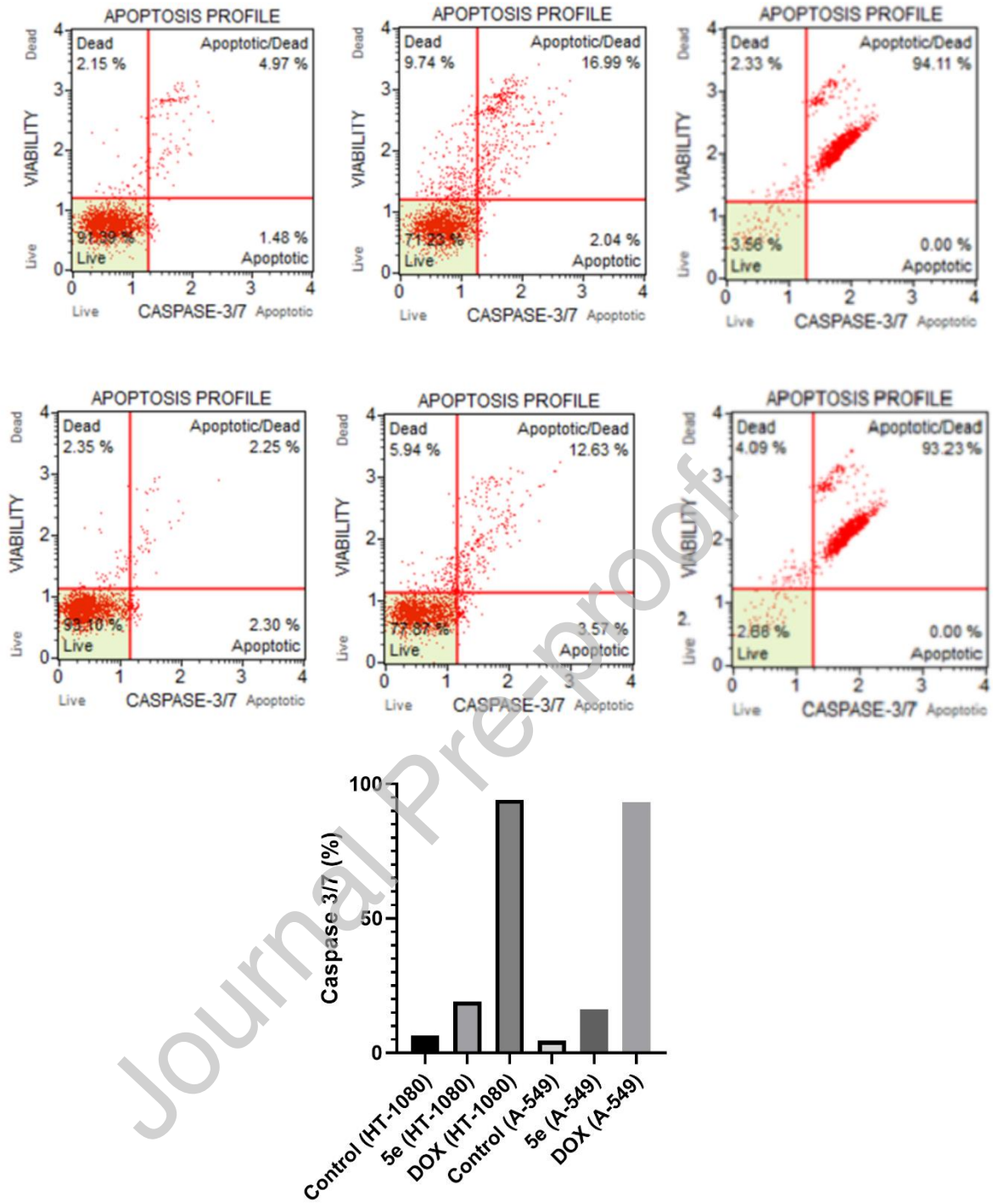

*Figure 3: Induction of caspase-3/7 activity in response to compound **5e**. HT-1080 and A-549 Cells were treated with 20 µM of desired compound as well as DMSO (control) for 24 hours.*

Effect of Compound 5e on cell cycle distribution

The effect of compound **5e** on cell cycle arrest in HT-1080 and A-549 cell lines was determined by flow cytometry. The selected cells were treated with 20 µM of **5e** and DMSO as control. The Analysis showed that compound **5e** induces arrest in the G2M phase of the

cell cycle. Indeed, the product decreases the rate of G2M from 14.14% and 13.0 to 18.7% and 15.8% in HT-1080 and A-549 cell lines, respectively (Fig. 3). Meanwhile, there was a significant increase in the rate of G2M in DOX-treated HT-108 and A-549 cancer cell lines; from 14.4 and 13% to 26.8% and 18%, respectively.

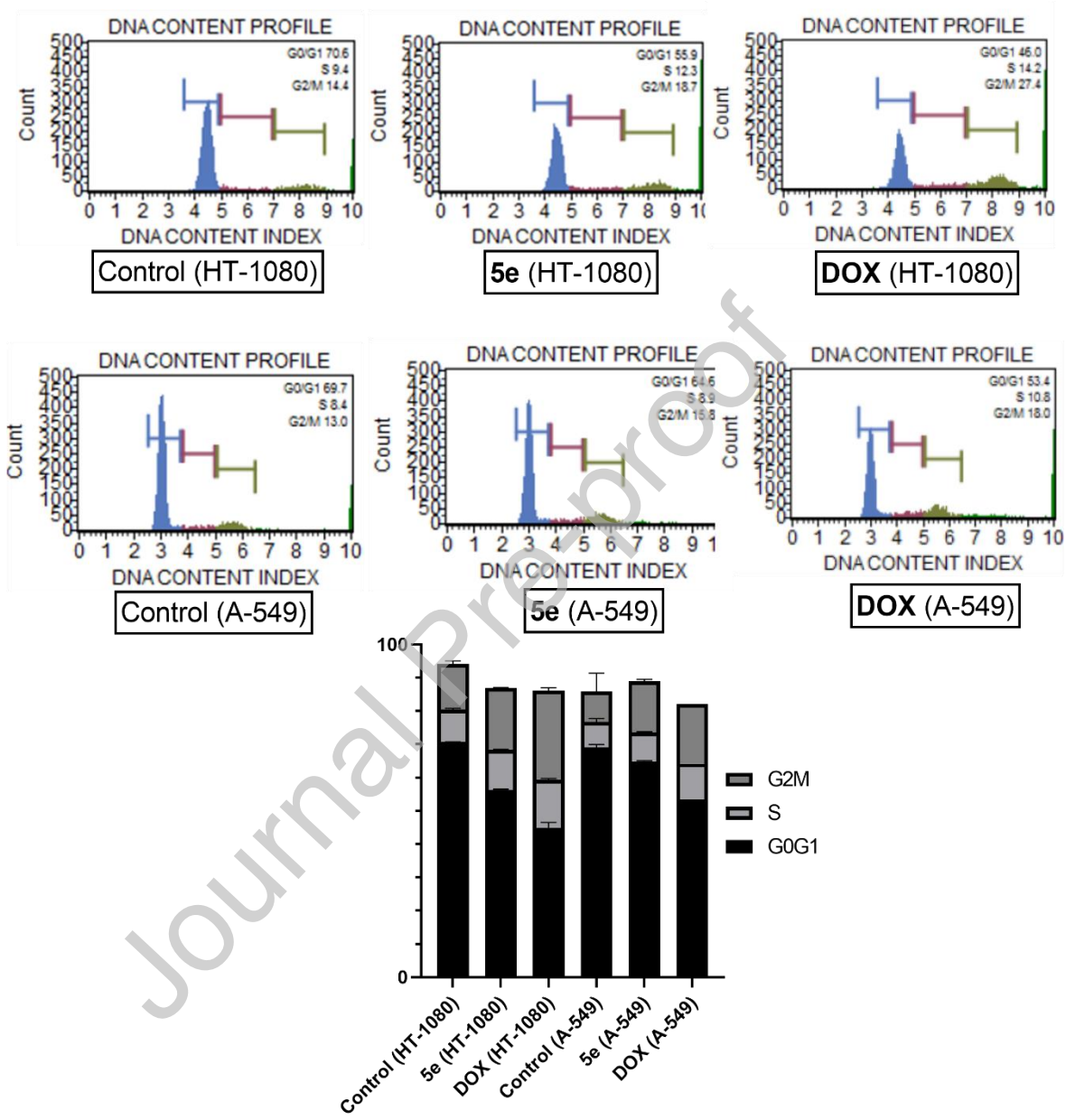

*Figure 4: Flow cytometry analysis of cell cycle phase distribution in HT-1080 and A-549 cell lines after treatment of 20 µM of compound **5e** in comparison with control for 24 hours.*

Molecular Docking

Considering the docking study of oxadiazole derivatives as potent caspase-3 activator [35, 60, 61], we have continued exploring the apoptosis induction through the caspase activation

using in-silico molecular docking. Thus, compound **5e** was docked into the active site of caspase-3 (PDB ID: 6CKZ). Prior to this, self-docking experiments were set-up to determine the validity of our docking protocol. The root-mean-square deviations (RMSD) between the predicted and the native poses were found to be 0.95 Å. These results indicated that the adopted docking protocol is acceptable for reproducing the native poses (<2 Å).

The docking results of the oxadiazole **5e, 5g,** and **5h** with caspase-3 are summarized in Figures 5-8 and table 2. The compounds **5e, 5g,** and **5h** could be docked into the active site of caspase-3 with the estimated free energies of binding of -7.8, -7.52, and -8.12 kcal/mol, respectively. Moreover, the estimated inhibition constant of compounds **5e, 5g,** and **5h** are 1.12, 3.09, and 1.12, respectively. Meanwhile, DOX has smaller binding energy (absolute value) than those of the investigated compounds. We could explain this by the fact that the DOX activates caspases by a different mechanism than the prepared products (it does not interact directly with caspase 3). Indeed, it was demonstrated that DOX-induced apoptosis is mainly initiated by oxidative DNA damage mediated by H_2O_2, leading to the $\Delta\Psi m$ increase and subsequent caspase-3 activation [62]. The 4-chlorophenyl moiety of product **5e** was surrounded by a partially hydrophobic cavity (Figure 5). The three synthesized compounds form hydrogen bonds with the caspase-3. Other interactions were also observed, such as Pi-cation, Pi-sulfur, Pi-Pi T-shaped, and Pi-alkyl. We notice that all ligands interact with the key amino acids ARG207, HIS121, GLN161, and Tyr204 (Fig 6). These results are in line with the literature, which stated that these interactions are fundamental for caspase-3 activation [35, 61, 63-67]. As a result, the promising activity of compounds **5e, 5g**, and **5h** could be mediated by binding to the active sites of caspase-3.

Table 2: Binding energy and inhibition constant of compounds **5e**, **5g**, **5h**, and DOX

Compounds	Binding Energy (Kcal/mol)	Inhibition constant (µM)
5e	-8.12	1.12
5g	-7.52	3.09
5h	-8.12	1.12
DOX	-6.05	37.5

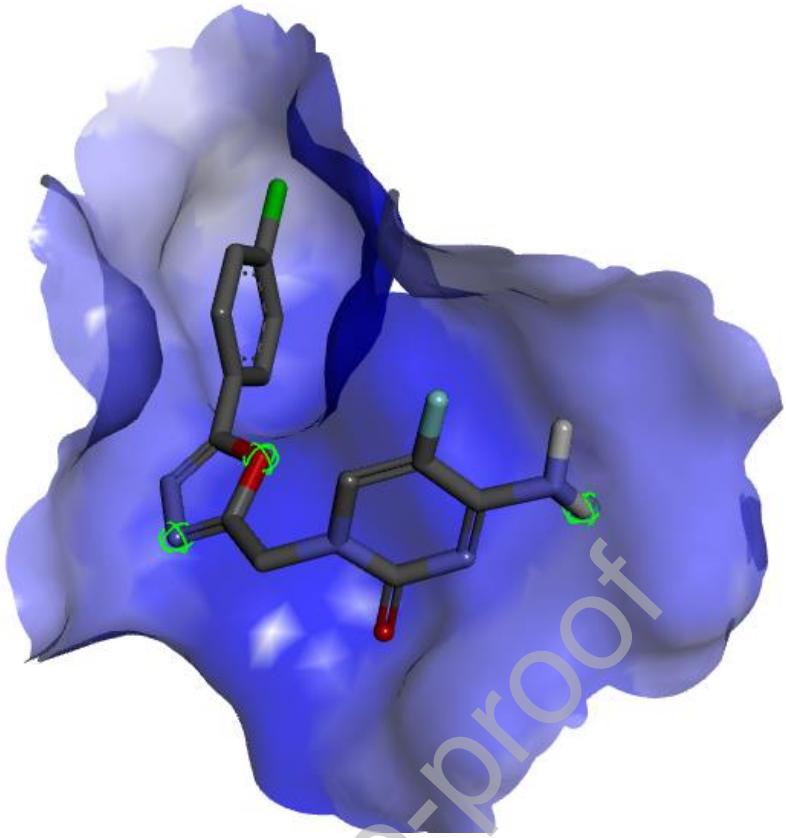

*Figure 5: The position of ligand **5e** in the hydrophobic cavity of caspase-3*

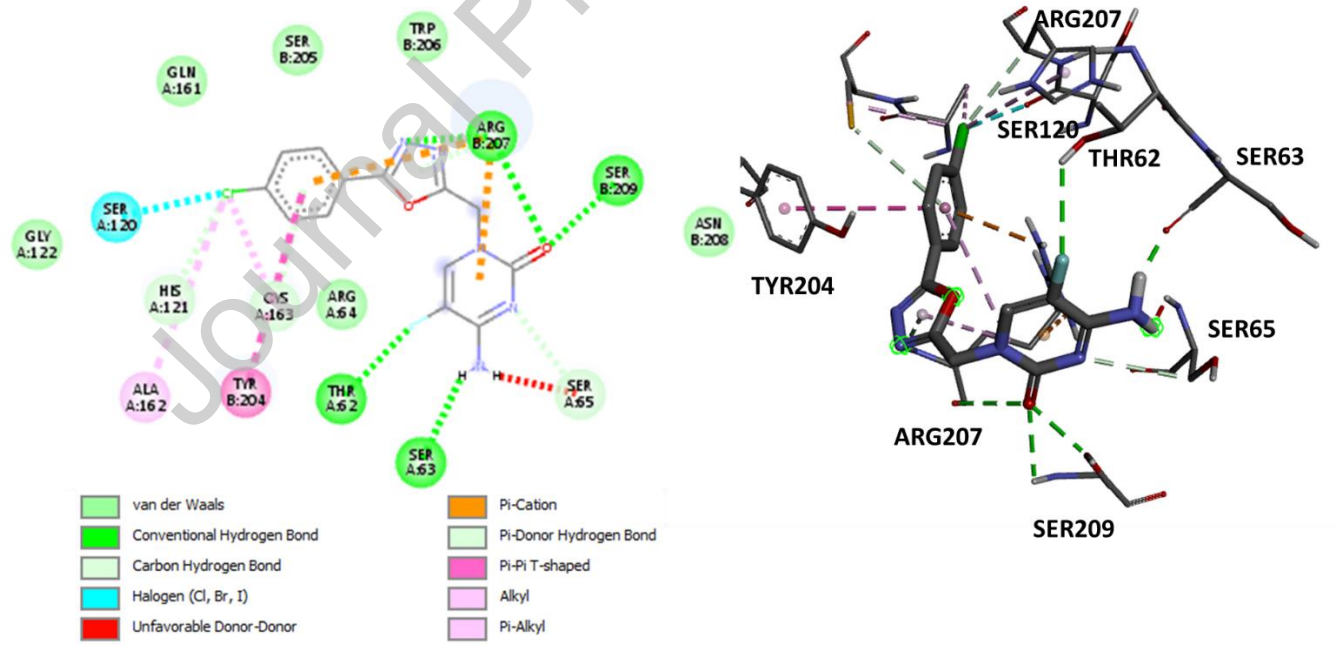

*Figure 6: 3D and 2D interactions of compound **5e** with the amino acid residues of caspase-3*

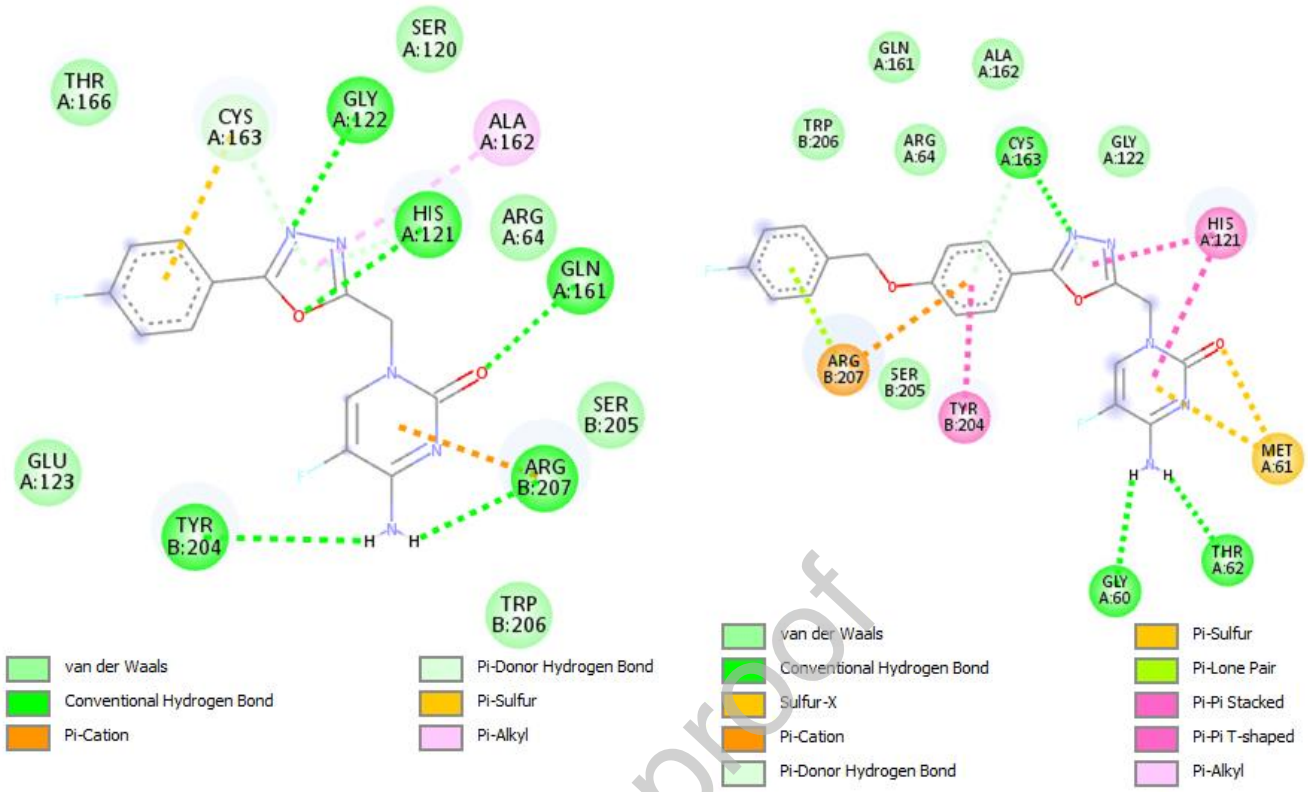

*Figure 7: 2D interactions of compounds **5g** and **5h** with the amino acid residues of caspase-3*

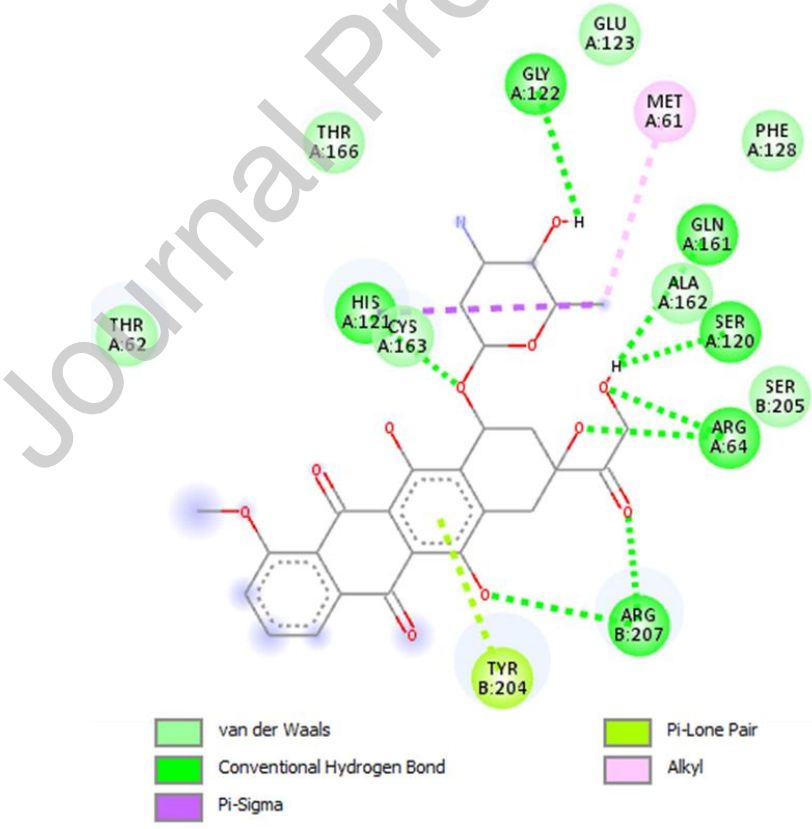

Figure 8: 2D interactions of DOX with the amino acid residues of caspase-3

Conclusion

A novel series of 5-fluorocytosine-1,3,4-oxadiazole conjugate derivatives were synthesized, fully characterized, and evaluated for their anticancer activities in HT-1080, A-549, MCF-7, and MDA-MB-23 cell lines. Among all synthesized derivatives, **5e** showed promising cytotoxic activity against HT-1080 cancer cell lines, with an IC_{50} value of 19.56 ± 1.62 µM. The mechanism of the anticancer activity on HT-1080 and A-549 was apoptotic by activation of caspase-3/7 with cell arrest at the G2M phase. Also, the molecular docking showed that compound **5e** entered deep inside the binding site of caspase-3 by forming *H*-bond, carbon-hydrogen bond, Pi-cation, Pi-sulfur, Pi-Pi T-shaped, and Pi-alkyl type non-covalent interactions.

In summary, 5-fluorocytosine-1,3,4-oxadiazole hybrid derivatives were successfully repurposed in this discovery research paper to act as promising anticancer agents. The findings of this study open new avenues for future research to synthesize more potent derivatives with improved pharmacokinetic properties.

Declaration of Competing Interest

The authors declare that they have no known competing financial interests or personal relationships that could have appeared to influence the work reported in this paper.

Acknowledgement

We thank Joost Schepers and Thibault Francken for their excellent technical assistance (Rega Institute for Medical Research). The authors would like to also thank the technical staff of the CAC (Centre of Analysis and Characterization), University Cadi Ayyad for running the spectroscopic analysis, and the Faculty of Sciences and Technologies Mohammedia, University Hassan II Casablanca.

CRediT authorship contribution statement

Az-eddine El Mansouri: Methodology, Writing – original draft, Software, Data curation. **Saida Lachhab:** Methodology, Writing – original draft, Data curation. **Ali Oubella:** Data curation, Formal analysis, Methodology. **Mehdi Ahmad:** Methodology, Writing – review & editing. **Johan Neyts:** Methodology, Writing – review & editing. **Dirk Jochmans:** Methodology, Writing – review & editing**. Winston Chiu:** Formal analysis. **Laura Vangeel:** Formal analysis**. Steven De Jonghe:** Formal analysis. **Hamid Morjani:** Data curation, Formal analysis, Methodology, Supervision, Writing – review & editing. **Mustapha Ait Ali:** Formal analysis, Supervision and Methodology. **Mohamed Zahouily:** Formal analysis, Supervision and Methodology. **Yogesh sanghvi :** Validation, Supervision, Writing – review & editing.

H.B.Lazrek: Conceptualization, Methodology, Project administration, Validation, Supervision, Writing – review & editing

References

[1] A. Jemal, R. Siegel, E. Ward, T. Murray, J. Xu, M.J. Thun, Cancer statistics, 2007, CA Cancer J Clin, 57 (2007) 43-66.
[2] Z. Moussa, M.A.M.S. El-Sharief, S.Y. Abbas, New imidazolidineiminothione derivatives: Synthesis, spectral characterization and evaluation of antitumor, antiviral, antibacterial and antifungal activities, European Journal of Medicinal Chemistry, 122 (2016) 419-428.
[3] C.B. Thompson, Apoptosis in the pathogenesis and treatment of disease, Science, 267 (1995) 1456-1462.
[4] D. Leung, G. Abbenante, D.P. Fairlie, Protease Inhibitors: Current Status and Future Prospects, Journal of Medicinal Chemistry, 43 (2000) 305-341.
[5] M.W. Boudreau, J. Peh, P.J. Hergenrother, Procaspase-3 Overexpression in Cancer: A Paradoxical Observation with Therapeutic Potential, ACS Chemical Biology, 14 (2019) 2335-2348.
[6] S. Storey, Targeting apoptosis: selected anticancer strategies, Nature Reviews Drug Discovery, 7 (2008) 971-972.
[7] K.L. Seley-Radtke, M.K. Yates, The evolution of nucleoside analogue antivirals: A review for chemists and non-chemists. Part 1: Early structural modifications to the nucleoside scaffold, Antiviral research, 154 (2018) 66-86.
[8] M.K. Yates, K.L. Seley-Radtke, The evolution of antiviral nucleoside analogues: A review for chemists and non-chemists. Part II: Complex modifications to the nucleoside scaffold, Antiviral research, 162 (2019) 5-21.
[9] A. Mahapatra, T. Prasad, T. Sharma, Pyrimidine: a review on anticancer activity with key emphasis on SAR, Future Journal of Pharmaceutical Sciences, 7 (2021) 123.
[10] R. Kaur, P. Kaur, S. Sharma, G. Singh, S. Mehndiratta, P.M. Bedi, K. Nepali, Anti-cancer pyrimidines in diverse scaffolds: a review of patent literature, Recent patents on anti-cancer drug discovery, 10 (2015) 23-71.
[11] A.M. Rabie, Potent Inhibitory Activities of the Adenosine Analogue Cordycepin on SARS-CoV-2 Replication, ACS Omega, 7 (2022) 2960-2969.
[12] A.M. Rabie, Efficacious Preclinical Repurposing of the Nucleoside Analogue Didanosine against COVID-19 Polymerase and Exonuclease, ACS Omega, 7 (2022) 21385-21396.
[13] P. Sharma, A. Kumar, M. Sharma, Synthesis and QSAR studies on 5-[2-(2-methylprop1-enyl)-1H benzimidazol-1yl]-4,6-diphenyl-pyrimidin-2-(5H)-thione derivatives as antibacterial agents, European Journal of Medicinal Chemistry, 41 (2006) 833-840.
[14] A. Bazgir, M.M. Khanaposhtani, A.A. Soorki, One-pot synthesis and antibacterial activities of pyrazolo[4',3':5,6]pyrido[2,3-d]pyrimidine-dione derivatives, Bioorganic & Medicinal Chemistry Letters, 18 (2008) 5800-5803.
[15] M. Johar, T. Manning, D.Y. Kunimoto, R. Kumar, Synthesis and in vitro anti-mycobacterial activity of 5-substituted pyrimidine nucleosides, Bioorganic & Medicinal Chemistry, 13 (2005) 6663-6671.
[16] O.A. Fathalla, S.M. Awad, M.S. Mohamed, Synthesis of new 2-thiouracil-5-sulphonamide derivatives with antibacterial and antifungal activity, Archives of Pharmacal Research, 28 (2005) 1205-1212.
[17] M. Li, N. Zhang, M. Li, Capecitabine treatment of HCT-15 colon cancer cells induces apoptosis via mitochondrial pathway, Tropical Journal of Pharmaceutical Research, 16 (2017) 1529-1536.
[18] A. Namvaran, M. Fazeli, S. Farajnia, G. Hamidian, H. Rezazadeh, Apoptosis and Caspase 3 Pathway Role on Anti-Proliferative Effects of Scrophulariaoxy Sepala Methanolic Extract on Caco-2 Cells, Drug research, 67 (2017) 547-552.

[19] M.R. Sadaie, R. Mayner, J. Doniger, A novel approach to develop anti-HIV drugs: adapting non-nucleoside anticancer chemotherapeutics, Antiviral research, 61 (2004) 1-18.
[20] J.H. Cho, F. Amblard, S.J. Coats, R.F. Schinazi, Synthesis of Cyclopentanyl Carbocyclic 5-Fluorocytosine ((−)-5-Fluorocarbodine) Using a Facially Selective Hydrogenation Approach, The Journal of Organic Chemistry, 78 (2013) 723-727.
[21] G. Verma, M.F. Khan, W. Akhtar, M.M. Alam, M. Akhter, M. Shaquiquzzaman, A Review Exploring Therapeutic Worth of 1,3,4-Oxadiazole Tailored Compounds, Mini Reviews in Medicinal Chemistry, 19 (2019) 477-509.
[22] Salahuddin, A. Mazumder, M.S. Yar, R. Mazumder, G.S. Chakraborthy, M.J. Ahsan, M.U. Rahman, Updates on synthesis and biological activities of 1,3,4-oxadiazole: A review, Synthetic Communications, 47 (2017) 1805-1847.
[23] H. Khalilullah, M. J. Ahsan, M. Hedaitullah, S. Khan, B. Ahmed, 1,3,4-Oxadiazole: A Biologically Active Scaffold, Mini Reviews in Medicinal Chemistry, 12 (2012) 789-801.
[24] J. Sun, J. A. Makawana, H.-L. Zhu, 1,3,4-Oxadiazole Derivatives as Potential Biological Agents, Mini Reviews in Medicinal Chemistry, 13 (2013) 1725-1743.
[25] C.E. Stecoza, G.M. Nitulescu, C. Draghici, M.T. Caproiu, O.T. Olaru, M. Bostan, M. Mihaila, Synthesis and Anticancer Evaluation of New 1,3,4-Oxadiazole Derivatives, 14 (2021) 438.
[26] J. Zhang, X. Wang, J. Yang, L. Guo, X. Wang, B. Song, W. Dong, W. Wang, Novel diosgenin derivatives containing 1,3,4-oxadiazole/thiadiazole moieties as potential antitumor agents: Design, synthesis and cytotoxic evaluation, European Journal of Medicinal Chemistry, 186 (2020) 111897.
[27] W. Liang, W. Guan, R. Chen, W. Wang, J. Li, K. Xu, C. Li, Q. Ai, W. Lu, H. Liang, S. Li, J. He, Cancer patients in SARS-CoV-2 infection: a nationwide analysis in China, Lancet Oncol, 21 (2020) 335-337.
[28] L. Zhang, F. Zhu, L. Xie, C. Wang, J. Wang, R. Chen, P. Jia, H.Q. Guan, L. Peng, Y. Chen, P. Peng, P. Zhang, Q. Chu, Q. Shen, Y. Wang, S.Y. Xu, J.P. Zhao, M. Zhou, Clinical characteristics of COVID-19-infected cancer patients: a retrospective case study in three hospitals within Wuhan, China, Annals of Oncology, 31 (2020) 894-901.
[29] H.O. Al-Shamsi, W. Alhazzani, A. Alhuraiji, E.A. Coomes, R.F. Chemaly, M. Almuhanna, R.A. Wolff, N.K. Ibrahim, M.L.K. Chua, S.J. Hotte, B.M. Meyers, T. Elfiki, G. Curigliano, C. Eng, A. Grothey, C. Xie, A Practical Approach to the Management of Cancer Patients During the Novel Coronavirus Disease 2019 (COVID-19) Pandemic: An International Collaborative Group, The Oncologist, 25 (2020) e936-e945.
[30] J. Bi, H. Ma, D. Zhang, J. Huang, D. Yang, Y. Wang, V. Verma, T. Zhang, D. Hu, Q. Mei, G. Han, J. Li, Does chemotherapy reactivate SARS-CoV-2 in cancer patients recovered from prior COVID-19 infection?, 56 (2020) 2002672.
[31] A.M. Rabie, Two antioxidant 2,5-disubstituted-1,3,4-oxadiazoles (CoViTris2020 and ChloViD2020): successful repurposing against COVID-19 as the first potent multitarget anti-SARS-CoV-2 drugs, New Journal of Chemistry, 45 (2021) 761-771.
[32] A.M. Rabie, CoViTris2020 and ChloViD2020: a striking new hope in COVID-19 therapy, Molecular Diversity, 25 (2021) 1839-1854.
[33] A.-e. El Mansouri, A. Oubella, K. Dânoun, M. Ahmad, J. Neyts, D. Jochmans, R. Snoeck, G. Andrei, H. Morjani, M. Zahouily, H.B. Lazrek, Discovery of novel furo[2,3-d]pyrimidin-2-one–1,3,4-oxadiazole hybrid derivatives as dual antiviral and anticancer agents that induce apoptosis, Archiv der Pharmazie, 354 (2021) 2100146.
[34] A.-e. El Mansouri, A. Oubella, A. Mehdi, M.Y. AitItto, M. Zahouily, H. Morjani, H.B. Lazrek, Design, synthesis, biological evaluation and molecular docking of new 1,3,4-oxadiazole homonucleosides and their double-headed analogs as antitumor agents, Bioorganic Chemistry, 108 (2021) 104558.
[35] A.-E. El Mansouri, A. Oubella, M. Maatallah, M.Y. AitItto, M. Zahouily, H. Morjani, H.B. Lazrek, Design, synthesis, biological evaluation and molecular docking of new uracil analogs-1,2,4-oxadiazole hybrids as potential anticancer agents, Bioorganic & Medicinal Chemistry Letters, 30 (2020) 127438.
[36] A.-E. El Mansouri, M. Maatallah, H. Ait Benhassou, A. Moumen, A. Mehdi, R. Snoeck, G. Andrei, M. Zahouily, H.B. Lazrek, Design, synthesis, chemical characterization, biological evaluation, and

docking study of new 1,3,4-oxadiazole homonucleoside analogs, Nucleosides, Nucleotides & Nucleic Acids, 39 (2020) 1088-1107.
[37] R. Boudewijns, H.J. Thibaut, S.J.F. Kaptein, R. Li, V. Vergote, L. Seldeslachts, J. Van Weyenbergh, C. De Keyzer, L. Bervoets, S. Sharma, L. Liesenborghs, J. Ma, S. Jansen, D. Van Looveren, T. Vercruysse, X. Wang, D. Jochmans, E. Martens, K. Roose, D. De Vlieger, B. Schepens, T. Van Buyten, S. Jacobs, Y. Liu, J. Martí-Carreras, B. Vanmechelen, T. Wawina-Bokalanga, L. Delang, J. Rocha-Pereira, L. Coelmont, W. Chiu, P. Leyssen, E. Heylen, D. Schols, L. Wang, L. Close, J. Matthijnssens, M. Van Ranst, V. Compernolle, G. Schramm, K. Van Laere, X. Saelens, N. Callewaert, G. Opdenakker, P. Maes, B. Weynand, C. Cawthorne, G. Vande Velde, Z. Wang, J. Neyts, K. Dallmeier, STAT2 signaling restricts viral dissemination but drives severe pneumonia in SARS-CoV-2 infected hamsters, Nature Communications, 11 (2020) 5838.
[38] T. Ivens, C. Van den Eynde, K. Van Acker, E. Nijs, G. Dams, E. Bettens, A. Ohagen, R. Pauwels, K. Hertogs, Development of a homogeneous screening assay for automated detection of antiviral agents active against severe acute respiratory syndrome-associated coronavirus, Journal of virological methods, 129 (2005) 56-63.
[39] T.N.D. Do, K. Donckers, L. Vangeel, A.K. Chatterjee, P.A. Gallay, M.D. Bobardt, J.P. Bilello, T. Cihlar, S. De Jonghe, J. Neyts, D. Jochmans, A robust SARS-CoV-2 replication model in primary human epithelial cells at the air liquid interface to assess antiviral agents, Antiviral research, 192 (2021) 105122.
[40] R. Abdelnabi, C.S. Foo, D. Jochmans, L. Vangeel, S. De Jonghe, P. Augustijns, R. Mols, B. Weynand, T. Wattanakul, R.M. Hoglund, The oral protease inhibitor (PF-07321332) protects Syrian hamsters against infection with SARS-CoV-2 variants of concern, J bioRxiv, (2021).
[41] R.L. Hoffman, R.S. Kania, M.A. Brothers, J.F. Davies, R.A. Ferre, K.S. Gajiwala, M. He, R.J. Hogan, K. Kozminski, L.Y. Li, J.W. Lockner, J. Lou, M.T. Marra, L.J. Mitchell, B.W. Murray, J.A. Nieman, S. Noell, S.P. Planken, T. Rowe, K. Ryan, G.J. Smith, J.E. Solowiej, C.M. Steppan, B. Taggart, Discovery of Ketone-Based Covalent Inhibitors of Coronavirus 3CL Proteases for the Potential Therapeutic Treatment of COVID-19, Journal of Medicinal Chemistry, 63 (2020) 12725-12747.
[42] G.M. Morris, R. Huey, W. Lindstrom, M.F. Sanner, R.K. Belew, D.S. Goodsell, A.J. Olson, AutoDock4 and AutoDockTools4: Automated docking with selective receptor flexibility, Journal of computational chemistry, 30 (2009) 2785-2791.
[43] A. Oubella, A. Bimoussa, S. Byadi, Y. Laamari, M. Fawzi, A. N'ait ousidi, D. Oblak, A. Auhmani, A. Riahi, H. Morjani, M.Y. Ait Itto, Cytotoxic and apoptotic effects of some (R)-carvone-isoxazoline derivatives on human fibrosarcoma and carcinoma cells: experimental evaluation for cytotoxicity, molecular docking and molecular dynamics studies, Journal of Biomolecular Structure and Dynamics, (2022) 1-14.
[44] A. Solania, G.E. González-Páez, D.W. Wolan, Selective and Rapid Cell-Permeable Inhibitor of Human Caspase-3, ACS Chemical Biology, 14 (2019) 2463-2470.
[45] L. Baddi, D. Ouzebla, A.-E. El Mansouri, M. Smietana, J.-J. Vasseur, H.B. Lazrek, Efficient one-pot, three-component procedure to prepare new α-aminophosphonate and phosphonic acid acyclic nucleosides, Nucleosides, Nucleotides & Nucleic Acids, 40 (2021) 43-67.
[46] A.-E.E. Mansouri, M. Zahouily, H.B. Lazrek, HMDS/KI a simple, a cheap and efficient catalyst for the one-pot synthesis of N-functionalized pyrimidines, Synthetic Communications, 49 (2019) 1802-1812.
[47] A. Oubella, A. Bimoussa, A. N'ait Oussidi, M. Fawzi, A. Auhmani, H. Morjani, A. Riahi, M.h. Esseffar, C. Parish, M.Y. Ait Itto, New 1,2,3-Triazoles from (R)-Carvone: Synthesis, DFT Mechanistic Study and In Vitro Cytotoxic Evaluation, 27 (2022) 769.
[48] A. Bimoussa, A. Oubella, M.E. Hachim, M. Fawzi, M.Y.A. Itto, O. Mentre, E.M. Ketatni, L. Bahsis, H. Morjani, A. Auhmani, New enaminone sesquiterpenic: TiCl4-catalyzed synthesis, spectral characterization, crystal structure, Hirshfeld surface analysis, DFT studies and cytotoxic activity, Journal of Molecular Structure, 1241 (2021) 130622.

[49] A. Oubella, M. Fawzi, A. Bimoussa, A. N'Ait Ousidi, A. Auhmani, A. Riahi, A. Robert, L. El Firdoussi, H. Morjani, M.Y. Ait Itto, Convenient route to benzo[1,2,3]selenadiazole–isoxazole hybrids and evaluation of their in vitro cytotoxicity, Chemical Papers, (2022).
[50] A. Zumla, J.F.W. Chan, E.I. Azhar, D.S.C. Hui, K.-Y. Yuen, Coronaviruses — drug discovery and therapeutic options, Nature Reviews Drug Discovery, 15 (2016) 327-347.
[51] L.B. Dustin, B. Bartolini, M.R. Capobianchi, M. Pistello, Hepatitis C virus: life cycle in cells, infection and host response, and analysis of molecular markers influencing the outcome of infection and response to therapy, Clinical Microbiology and Infection, 22 (2016) 826-832.
[52] A.A. Elfiky, Ribavirin, Remdesivir, Sofosbuvir, Galidesivir, and Tenofovir against SARS-CoV-2 RNA dependent RNA polymerase (RdRp): A molecular docking study, Life Sciences, 253 (2020) 117592.
[53] T.L. Parsons, L.A. Kryszak, M.A. Marzinke, Development and validation of assays for the quantification of β-D-N4-hydroxycytidine in human plasma and β-D-N4-hydroxycytidine-triphosphate in peripheral blood mononuclear cell lysates, Journal of Chromatography B, 1182 (2021) 122921.
[54] A.J.W. te Velthuis, Common and unique features of viral RNA-dependent polymerases, Cellular and Molecular Life Sciences, 71 (2014) 4403-4420.
[55] E.D. Clercq, G. Li, Approved Antiviral Drugs over the Past 50 Years, 29 (2016) 695-747.
[56] C.J. Gordon, E.P. Tchesnokov, E. Woolner, J.K. Perry, J.Y. Feng, D.P. Porter, M. Götte, Remdesivir is a direct-acting antiviral that inhibits RNA-dependent RNA polymerase from severe acute respiratory syndrome coronavirus 2 with high potency, Journal of Biological Chemistry, 295 (2020) 6785-6797.
[57] L. Tian, Z. Pang, M. Li, F. Lou, X. An, S. Zhu, L. Song, Y. Tong, H. Fan, J.J.F.I. Fan, Molnupiravir and Its Antiviral Activity Against COVID-19, 13 (2022).
[58] F. Kabinger, C. Stiller, J. Schmitzová, C. Dienemann, G. Kokic, H.S. Hillen, C. Höbartner, P. Cramer, Mechanism of molnupiravir-induced SARS-CoV-2 mutagenesis, Nature Structural & Molecular Biology, 28 (2021) 740-746.
[59] C. Praveen Kumar, T.S. Reddy, P.S. Mainkar, V. Bansal, R. Shukla, S. Chandrasekhar, H.M. Hügel, Synthesis and biological evaluation of 5,10-dihydro-11H-dibenzo[b,e][1,4]diazepin-11-one structural derivatives as anti-cancer and apoptosis inducing agents, European Journal of Medicinal Chemistry, 108 (2016) 674-686.
[60] A. Vaidya, A.K. Jain, B.R. Prashantha Kumar, G.N. Sastry, S.K. Kashaw, R.K. Agrawal, CoMFA, CoMSIA, kNN MFA and docking studies of 1,2,4-oxadiazole derivatives as potent caspase-3 activators, Arabian Journal of Chemistry, 10 (2017) S3936-S3946.
[61] A.-e. El Mansouri, A. Oubella, A. Mehdi, M.Y. AitItto, M. Zahouily, H. Morjani, H.B. Lazrek, Design, synthesis, biological evaluation and molecular docking of new 1,3,4-oxadiazole homonucleosides and their double-headed analogs as antitumor agents, Bioorganic Chemistry, (2020) 104558.
[62] H. Mizutani, S. Tada-Oikawa, Y. Hiraku, M. Kojima, S. Kawanishi, Mechanism of apoptosis induced by doxorubicin through the generation of hydrogen peroxide, Life Sciences, 76 (2005) 1439-1453.
[63] M. Pandurangan, G. Enkhtaivan, D.H. Kim, Therapeutic efficacy of natural dipeptide carnosine against human cervical carcinoma cells, Journal of Molecular Recognition, 29 (2016) 426-435.
[64] R. Mutazah, H.A. Hamid, A.N. Mazila Ramli, M.F. Fasihi Mohd Aluwi, M.M. Yusoff, In vitro cytotoxicity of Clinacanthus nutans fractions on breast cancer cells and molecular docking study of sulphur containing compounds against caspase-3, Food and Chemical Toxicology, 135 (2020) 110869.
[65] I.M. Abdel-Rahman, M. Mustafa, S.A. Mohamed, R. Yahia, M. Abdel-Aziz, G.E.-D.A. Abuo-Rahma, A.M. Hayallah, Novel Mannich bases of ciprofloxacin with improved physicochemical properties, antibacterial, anticancer activities and caspase-3 mediated apoptosis, Bioorganic Chemistry, 107 (2021) 104629.
[66] A. Oubella, A.-E. El Mansouri, M. Fawzi, A. Bimoussa, Y. Laamari, A. Auhmani, H. Morjani, A. Robert, A. Riahi, M. Youssef Ait Itto, Thiazolidinone-linked1,2,3-triazoles with monoterpenic skeleton as new potential anticancer agents: Design, synthesis and molecular docking studies, Bioorganic Chemistry, 115 (2021) 105184.

[67] Y. Laamari, A. Oubella, A. Bimoussa, A.-E. El Mansouri, E.M. Ketatni, O. Mentre, M.Y. Ait Itto, H. Morjani, M. Khouili, A. Auhmani, Design, Hemiysnthesis, crystal structure and anticancer activity of 1, 2, 3-triazoles derivatives of totarol, Bioorganic Chemistry, 115 (2021) 105165.

Graphical abstract